Inorg. Chem. **2008**, *47*, 9055−9068

Near-Infrared Luminescence of Nine-Coordinate Neodymium Complexes with Benzimidazole-Substituted 8-Hydroxyquinolines

Nail M. Shavaleev, Rosario Scopelliti, Frédéric Gumy, and Jean-Claude G. Bünzli*

École Polytechnique Fédérale de Lausanne, Laboratory of Lanthanide Supramolecular Chemistry, BCH 1405, CH-1015 Lausanne, Switzerland

Received June 9, 2008

A new class of benzimidazole-substituted 8-hydroxyquinoline ligands has been prepared that contain a monoanionic tridentate N,N,O-coordinating unit. These ligands form charge-neutral lanthanide complexes of the type $[Ln(L\text{-}R)_3]\cdot nH_2O$ or $[Ln_2(L2)_3]\cdot nH_2O$ ($n = 1-3$) with early lanthanides from La^{III} to Gd^{III} inclusive. Crystallographic characterization was carried out for 11 complexes with 6 different ligands. In all of these structures, the lanthanide ion was found to be nine-coordinated by three ligands arranged in an "up−up−down" fashion around the metal center. The coordination environment can be described as a tricapped trigonal prism, with N atoms of quinoline rings occupying capping positions. Upon deprotonation of the ligand and complex formation, a new absorption band appears in the visible range of the spectrum with a maximum in the range of 466−483 nm and molar absorption coefficient of $(7.2 - 18) \times 10^3\ M^{-1}\ cm^{-1}$. Its origin is likely to be an intraligand phenolate-to-pyridyl charge transfer transition centered on the 8-hydroxyquinolate chromophore. Upon excitation in ligand absorption bands, new Nd^{III} complexes display characteristic metal-centered luminescence in the near-infrared region from 850 to 1450 nm with quantum yields and lifetimes in solid state at room temperature as high as 0.34% and 1.2 μs, respectively.

Introduction

8-Hydroxyquinolines form stable complexes with a variety of metal[1−7] and nonmetal[8] elements. These complexes often display efficient luminescence[2−8] that can be adjusted in color from blue to infrared by modification of the ligand or by choice of the adequate element. As a result, in the past 20 years, 8-hydroxyquinolate complexes have been intensely developed for OLED and display technologies.[9−11] Lanthanide ions also form stable complexes with 8-hydrox-

* To whom correspondence should be addressed. E-mail: jean-claude.bunzli@epfl.ch.

(1) (a) Albrecht, M.; Blau, O.; Witt, K.; Wegelius, E.; Nissinen, M.; Rissanen, K.; Fröhlich, R. *Synthesis* **1999**, 1819. (b) Deraeve, C.; Boldron, C.; Maraval, A.; Mazarguil, H.; Gornitzka, H.; Vendier, L.; Pitie, M.; Meunier, B. *Chem.—Eur. J.* **2008**, *14*, 682.

(2) (a) Ballardini, R.; Varani, G.; Indelli, M. T.; Scandola, F. *Inorg. Chem.* **1986**, *25*, 3858. (b) Donges, D.; Nagle, J. K.; Yersin, H. *Inorg. Chem.* **1997**, *36*, 3040.

(3) (a) Pearce, D. A.; Jotterand, N.; Carrico, I. S.; Imperiali, B. *J. Am. Chem. Soc.* **2001**, *123*, 5160. (b) Ghedini, M.; La Deda, M.; Aiello, I.; Grisolia, A. *Inorg. Chim. Acta* **2004**, *357*, 33. (c) Montes, V. A.; Pohl, R.; Shinar, J.; Anzenbacher, P., Jr. *Chem.—Eur. J.* **2006**, *12*, 4523. (d) Royzen, M.; Durandin, A.; Young, V. G., Jr.; Geacintov, N. E.; Canary, J. W. *J. Am. Chem. Soc.* **2006**, *128*, 3854. (e) Kappaun, S.; Eder, S.; Sax, S.; Mereiter, K.; List, E. J. W.; Slugovc, C. *Eur. J. Inorg. Chem.* **2007**, 4207. (f) Wang, J.; Oyler, K. D.; Bernhard, S. *Inorg. Chem.* **2007**, *46*, 5700.

(4) Katkova, M. A.; Kurskii, Y. A.; Fukin, G. K.; Averyushkin, A. S.; Artamonov, A. N.; Vitukhnovsky, A. G.; Bochkarev, M. N. *Inorg. Chim. Acta* **2005**, *358*, 3625.

(5) Ouyang, J.; Li, L.; Tai, Z.; Lu, Z.; Wang, G. *Chem. Commun.* **1997**, 815.

(6) Iwamuro, M.; Adachi, T.; Wada, Y.; Kitamura, T.; Nakashima, N.; Yanagida, S. *Bull. Chem. Soc. Jpn.* **2000**, *73*, 1359.

(7) (a) Magennis, S. W.; Ferguson, A. J.; Bryden, T.; Jones, T. S.; Beeby, A.; Samuel, I. D. W. *Synth. Met.* **2003**, *138*, 463. (b) Suzuki, H.; Hattori, Y.; Iizuka, T.; Yuzawa, K.; Matsumoto, N. *Thin Solid Films* **2003**, *438−439*, 288. (c) Park, O.-H.; Seo, S.-Y.; Bae, B.-S.; Shin, J. H. *Appl. Phys. Lett.* **2003**, *82*, 2787. (d) Thompson, J.; Blyth, R. I. R.; Gigli, G.; Cingolani, R. *Adv. Funct. Mater.* **2004**, *14*, 979. (e) Penna, S.; Reale, A.; Pizzoferrato, R.; Tosi Beleffi, G. M.; Musella, D.; Gillin, W. P. *Appl. Phys. Lett.* **2007**, *91*, 021106/1. (f) Van Deun, R.; Fias, P.; Nockemann, P.; Van Hecke, K.; Van Meervelt, L.; Binnemans, K. *Eur. J. Inorg. Chem.* **2007**, 302.

(8) Cui, Y.; Liu, Q. D.; Bai, D. R.; Jia, W. L.; Tao, Y.; Wang, S. *Inorg. Chem.* **2005**, *44*, 601.

(9) (a) Katkova, M. A.; Vitukhnovsky, A. G.; Bochkarev, M. N. *Russ. Chem. Rev.* **2005**, *74*, 1089. (b) de Bettencourt-Dias, A. *Dalton Trans.* **2007**, 2229.

(10) (a) Tang, C. W.; VanSlyke, S. A. *Appl. Phys. Lett.* **1987**, *51*, 913. (b) Sapochak, L. S.; Benincasa, F. E.; Schofield, R. S.; Baker, J. L.; Riccio, K. K. C.; Fogarty, D.; Kohlmann, H.; Ferris, K. F.; Burrows, P. E. *J. Am. Chem. Soc.* **2002**, *124*, 6119. (c) Yi, C.; Yang, C.-J.; Liu, J.; Xu, M.; Wang, J.-H.; Cao, Q.-Y.; Gao, X.-C. *Inorg. Chim. Acta* **2007**, *360*, 3493.

10.1021/ic8010585 CCC: $40.75
Published on Web 08/22/2008

yquinolines.[4,6,7,12] The corresponding La^{III} complexes display ligand-centered fluorescence,[4,5] while Nd^{III}, Er^{III}, and Yb^{III} complexes display metal-centered near-infrared luminescence.[6,7] Recently, complexes with Nd^{III}, Er^{III}, and Yb^{III} ions have gained interest for biochemical analysis[13] and in telecommunications technology[14] because infrared emission lines of these ions coincide with a transparency window of biological tissues and silica optical fibers.[15−18]

Lanthanide ions prefer high coordination numbers, with 8 or 9 being the most common ones.[19] 8-Hydroxyquinolines are bidentate monoanionic ligands and thus cannot saturate the coordination sphere of a lanthanide ion upon formation of a charge-neutral tris-complex. In addition, the hydroxy group in these ligands tends to act as a bridge in lanthanide complexes. As a result, attempted syntheses of lanthanide complexes with bidentate 8-hydroxyquinolines often give mixtures of mono- and polynuclear complexes.[12] To make the outcome of synthesis more predictable, it is advantageous to employ polydentate 8-hydroxyquinolines for coordination with lanthanides.[5,20−23] Our group has recently developed encapsulating polydentate podates based on 8-hydroxyquinolines which form water-stable and water-soluble lanthanide complexes.[20] In another approach, amide-modified tridentate 8-hydroxyquinolines were used to form charge-neutral mononuclear tris-complexes with lanthanides (Chart 1, top structure).[5,21] In this work we describe the synthesis of lanthanide complexes with a new series of tridentate ligands based on benzimidazole-substituted 8-hydroxyquinolines (Scheme 1), as well as the luminescent properties of the corresponding La^{III} and Nd^{III} chelates. It should be noted that several types of tridentate ligands based on 8-hydroxyquinolines were developed previously;[5,21,24−26] however only the amide-modified ones were coordinated to lanthanides (Chart 1).[5,21]

Chart 1. Tridentate Monoanionic Ligands Based on 8-Hydroxyquinoline[5,21,24−26] Known from Previous Studies[a]

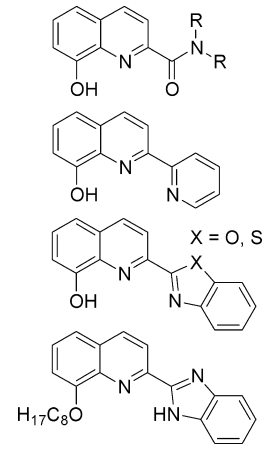

[a] Lanthanide complexes have only been reported for amide-modified ligands (top structure).[5,21]

Results and Discussion

Synthesis. The ligands were prepared by a modified general method of benzimidazole ring synthesis described by Yang et al.[27] It involves a reaction of substituted *N*-alkyl-2-nitroaniline with aldehyde (in our case, 8-hydroxyquinoline-2-carboxaldehyde) in the presence of $Na_2S_2O_4$ as a reducing agent (Scheme 1). The synthesis was carried out at 100 °C in solvent mixtures of either DMF/H_2O or 2-methoxyethanol/H_2O; attempts to perform this reaction at lower temperatures or in the absence of water gave intricate mixtures of products. The advantage of this synthetic

(11) (a) Khreis, O. M.; Curry, R. J.; Somerton, M.; Gillin, W. P. *J. Appl. Phys.* **2000**, *88*, 777. (b) Zhao, W. Q.; Ran, G. Z.; Ma, G. L.; Xu, W. J.; Dai, L.; Liu, W. M.; Wang, P. F.; Qin, G. G. *Appl. Phys. Lett.* **2006**, *89*, 022109/1.
(12) (a) Van Deun, R.; Fias, P.; Nockemann, P.; Schepers, A.; Parac-Vogt, T. N.; Van Hecke, K.; Van Meervelt, L.; Binnemans, K. *Inorg. Chem.* **2004**, *43*, 8461. (b) Leary, S. G.; Deacon, G. B.; Junk, P. C. *Z. Anorg. Allg. Chem.* **2005**, *631*, 2647. (c) Artizzu, F.; Marchio, L.; Mercuri, M. L.; Pilia, L.; Serpe, A.; Quochi, F.; Orru, R.; Cordella, F.; Saba, M.; Mura, A.; Bongiovanni, G.; Deplano, P. *Adv. Funct. Mater.* **2007**, *17*, 2365.
(13) (a) Gaiduk, M. I.; Grigoryants, V. V.; Mironov, A. F.; Rumyantseva, V. D.; Chissov, V. I.; Sukhin, G. M. *J. Photochem. Photobiol., B: Biol.* **1990**, *7*, 15. (b) Horrocks, W. D. W., Jr.; Bolender, J. P.; Smith, W. D.; Supkowski, R. M. *J. Am. Chem. Soc.* **1997**, *119*, 5972. (c) Beeby, A.; Dickins, R. S.; FitzGerald, S.; Govenlock, L. J.; Parker, D.; Williams, J. A. G.; Maupin, C. L.; Riehl, J. P.; Siligardi, G. *Chem. Commun.* **2000**, 1183. (d) Werts, M. H. V.; Woudenberg, R. H.; Emmerink, P. G.; van Gassel, R.; Hofstraat, J. W.; Verhoeven, J. W. *Angew. Chem., Int. Ed.* **2000**, *39*, 4542.
(14) (a) Polman, A.; van Veggel, F. C. J. M. *J. Opt. Soc. Am. B* **2004**, *21*, 871. (b) Riman, R. E.; Kumar, G. A.; Banerjee, S.; Brennan, J. G. *J. Am. Ceram. Soc.* **2006**, *89*, 1809.
(15) Comby, S. ; Bünzli, J.-C. G. Lanthanide near-infrared luminescence in molecular probes and devices In *Handbook on the Physics and Chemistry of Rare Earths*; Gschneidner, J. A., Jr., Bünzli, J.-C. G., Pecharsky, V., Eds.; Elsevier Science B.V.: Amsterdam, 2007; Vol. *37*, Chapter 235, and references therein.
(16) Yanagida, S.; Hasegawa, Y.; Murakoshi, K.; Wada, Y.; Nakashima, N.; Yamanaka, T. *Coord. Chem. Rev.* **1998**, *171*, 461.
(17) (a) Rusakova, N. V.; Korovin, V. Yu.; Zhilina, Z. I.; Vodzinskii, S. V.; Ishkov, Yu. V. *J. Appl. Spectrosc.* **2004**, *71*, 506. (b) Ronson, T. K.; Lazarides, T.; Adams, H.; Pope, S. J. A.; Sykes, D.; Faulkner, S.; Coles, S. J.; Hursthouse, M. B.; Clegg, W.; Harrington, R. W.; Ward, M. D. *Chem.—Eur. J.* **2006**, *12*, 9299. (c) Xu, H.-B.; Zhang, L.-Y.; Xie, Z.-L.; Ma, E.; Chen, Z.-N. *Chem. Commun.* **2007**, 2744. (d) Glover, P. B.; Bassett, A. P.; Nockemann, P.; Kariuki, B. M.; Van Deun, R.; Pikramenou, Z. *Chem.—Eur. J.* **2007**, *13*, 6308. (e) Zhang, J.; Petoud, S. *Chem.—Eur. J.* **2008**, *14*, 1264. (f) Zheng, Y.; Motevalli, M.; Tan, R. H. C.; Abrahams, I.; Gillin, W. P.; Wyatt, P. B. *Polyhedron* **2008**, *27*, 1503.
(18) Ziessel, R.; Ulrich, G.; Charbonnière, L. J.; Imbert, D.; Scopelliti, R.; Bünzli, J.-C. G. *Chem.—Eur. J.* **2006**, *12*, 5060–5067.
(19) (a) Bünzli, J.-C. G.; Piguet, C. *Chem. Soc. Rev.* **2005**, *34*, 1048. (b) Gunnlaugsson, T.; Stomeo, F. *Org. Biomol. Chem.* **2007**, *5*, 1999.
(20) (a) Comby, S.; Imbert, D.; Chauvin, A.-S.; Bünzli, J.-C. G. *Inorg. Chem.* **2006**, *45*, 732. (b) Comby, S.; Imbert, D.; Vandevyver, C.; Bünzli, J.-C. G. *Chem.—Eur. J.* **2007**, *13*, 936.
(21) (a) Albrecht, M.; Osetska, O.; Klankermayer, J.; Fröhlich, R.; Gumy, F.; Bünzli, J.-C. G. *Chem. Commun.* **2007**, 1834. (b) Albrecht, M.; Osetska, O.; Fröhlich, R.; Bünzli, J.-C. G.; Aebischer, A.; Gumy, F.; Hamacek, J. *J. Am. Chem. Soc.* **2007**, *129*, 14178.
(22) (a) Arslan, T.; Ogretir, C.; Tsiouri, M.; Plakatouras, J. C.; Hadjiliadis, N. *J. Coord. Chem.* **2007**, *60*, 699. (b) Albrecht, M.; Mirtschin, S.; Osetska, O.; Dehn, S.; Enders, D.; Fröhlich, R.; Pape, T.; Hahn, E. F. *Eur. J. Inorg. Chem.* **2007**, 3276.
(23) Rizzo, F.; Papagni, A.; Meinardi, F.; Tubino, R.; Ottonelli, M.; Musso, G. F.; Dellepiane, G. *Synth. Met.* **2004**, *147*, 143.
(24) Corsini, A.; Cassidy, R. M. *Talanta* **1979**, *26*, 297.
(25) (a) Youk, J.-S.; Kim, Y. H.; Kim, E.-J.; Youn, N. J.; Chang, S.-K. *Bull. Korean Chem. Soc.* **2004**, *25*, 869. (b) Kim, J. S.; Choi, M. G.; Huh, Y.; Kim, M. H.; Kim, S. H.; Wang, S. Y.; Chang, S.-K. *Bull. Korean Chem. Soc.* **2006**, *27*, 2058. (c) Everson da Silva, L.; Joussef, A. C.; Foro, S.; Schmidt, B. *Acta Crystallogr.* **2006**, *E62*, o880.
(26) Li, S.; Lu, J.; Liang, H.; Han, S.; Zhou, X. *Inorg. Chem. Commun.* **2008**, *11*, 662.
(27) Yang, D.; Fokas, D.; Li, J.; Yu, L.; Baldino, C. M. *Synthesis* **2005**, 47.

Scheme 1. Synthesis and Structures of New Ligands[a]

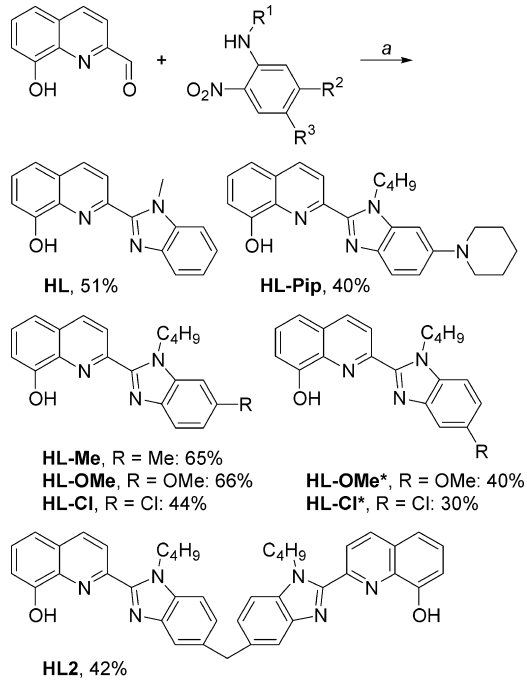

[a] Reaction conditions: (a) $Na_2S_2O_4$, DMF/H_2O or 2-methoxyethanol/H_2O, under N_2, 100°C.

procedure is that it does not require protection of the hydroxyl group of the 8-hydroxyquinoline moiety. The *N*-alkyl-2-nitroaniline precursors were prepared via a facile reaction of 2-halonitrobenzenes with primary alkyl amines;[28] even in the case of 2,4- and 2,5-dichloronitrobenzenes, the first amination occurs selectively at position 2, which allows for stepwise modification of the precursors (Scheme 2). In total, seven tridentate ligands and one bis-tridentate bridging ligand were prepared that carried various groups at positions 5/6 of benzimidazole ring (Scheme 1). They were obtained as white or pale yellow solids (apart from the intense yellow ligand HL-Pip) in yields ranging from 30 to 66%; in some cases, separation of a small amount of byproduct diminished the yields. All ligands were identified by elemental analysis and ^{1}H NMR spectroscopy (Figures S1−S12).

Lanthanide complexes were obtained as orange or red solids in 74−91% yields from ethanol/water solutions starting from $LnCl_3 \cdot nH_2O$ and using NaOH as a base. Elemental analyses confirmed the formulation of the complexes as $[Ln(L\text{-}R)_3] \cdot nH_2O$ or $[Ln_2(L2)_3] \cdot nH_2O$ containing up to three molecules of crystallization water (Chart 2). Lanthanide complexes with ligand HL could only be prepared for early lanthanides, from La^{III} to Gd^{III}, inclusive. Correct analytical results could not be obtained for the corresponding complexes of heavier lanthanides (Er^{III}, Yb^{III}), and these ions were not used further in this study. For the rest of the ligands, only La^{III} and Nd^{III} complexes were prepared to study their luminescence properties.

X-Ray Structural Data. The structures of ligand HL-Cl and 11 complexes with six different ligands were determined by X-ray crystallography (Table 1) and are presented in Figure 1 while selected structural parameters are collected in Table 2

Two independent molecules are found in the unit cell of ligand HL-Cl; one has a benzimidazole group rotated out of the plane of the quinoline moiety by 10.35°, while another is nearly planar with an angle between two groups of 3.45°. In both molecules, imine nitrogens of benzimidazole and quinoline groups are situated in trans position to each other. This probably minimizes electrostatic interaction of the lone pairs of the imine nitrogen atoms and also helps to avoid a steric clash of the 3-H atom on the quinoline ring with alkyl hydrogens of the benzimidazole *N*-*n*-butyl group.

The following properties are observed in all of the structures of the complexes (Figure 1, Table 2): (i) the lanthanide ion is nine-coordinated by three ligands arranged in an "up−up−down" fashion around the metal center; (ii) the coordination environment around the metal ion can be described as a distorted tricapped trigonal prism,[29] with N atoms of quinoline rings occupying capping positions (these N atoms lay perfectly in-plane with the Ln atom); (iii) the three ligands are not equally strongly bonded to the lanthanide as reflected in the different respective sets of bond lengths; (iv) ligands within one complex are not planar and dihedral angles between quinoline and benzimidazole groups vary from 4.78 to 44.14°; (v) within the series of complexes with ligand HL, the Ln−O and Ln−N bond lengths monotonously decrease from La, through Pr, Nd, Sm, and Eu as a result of lanthanide contraction; (vi) the lanthanide ion is preferentially bound to the 8-hydroxyquinoline (quin) group, while bonding to the benzimidazole (bzim) group is relatively weak, which is reflected in longer Ln−N(bzim) bond lengths and their wider variation in range. The latter statement is illustrated by the Nd^{III} complexes with ligands HL, HL-Cl, HL-OMe, HL-Cl*, and HL-OMe*, where the experimental bond lengths vary as follows: Nd−O, 2.334−2.457 Å (Δ = 0.123 Å); Nd−N(quin), 2.591−2.725 Å (Δ = 0.134 Å); Nd−N(bzim), 2.656−2.935 (Δ = 0.279 Å). In certain cases, the Ln−N(bzim) bond for one of the ligands in the complex is quite long (>2.8 Å), and the metal center may be considered as (8 + 1)-coordinate as opposed to 9-coordinate. No significant differences in structural parameters are observed between Nd^{III} complexes containing ligands substituted in 5- or 6-position of the benzimidazole ring, pointing to similar steric effects in these ligands.

In some structures of the complexes, the cocrystallized solvent molecules containing OH groups (ethanol or water) are found to be hydrogen-bonded to the oxygen atom of the 8-hydroxyquinoline ligand with O−H···O distances of <2.0 Å. This occurs in the following structures: for $[La(L)_3]$, $[Nd(L)_3]$, and $[Sm(L)_3]$, possible interaction with H_2O is pointed out, although hydrogen atoms on water could not be located; for $[Eu(L)_3]$ and $[Nd(L\text{-}Cl^*)_3]$, interaction with ethanol is observed; for $[Pr(L)_3]$, interaction with ethanol and two molecules of H_2O is found, each of these molecules

(28) Blatch, A. J.; Chetina, O. V.; Howard, J. A. K.; Patrick, L. G. F.; Smethurst, C. A.; Whiting, A. *Org. Biomol. Chem.* **2006**, *4*, 3297.

(29) Thompson, L. C. Complexes In *Handbook on the Physics and Chemistry of Rare Earths*; Gschneidner, K. A., Jr., Eyring, L., Eds.; North Holland Publ. Co.: Amsterdam, 1979; Vol. *3*, Chapter 25.

Scheme 2. Synthesis of *N*-Alkyl-2-nitroanilines[a]

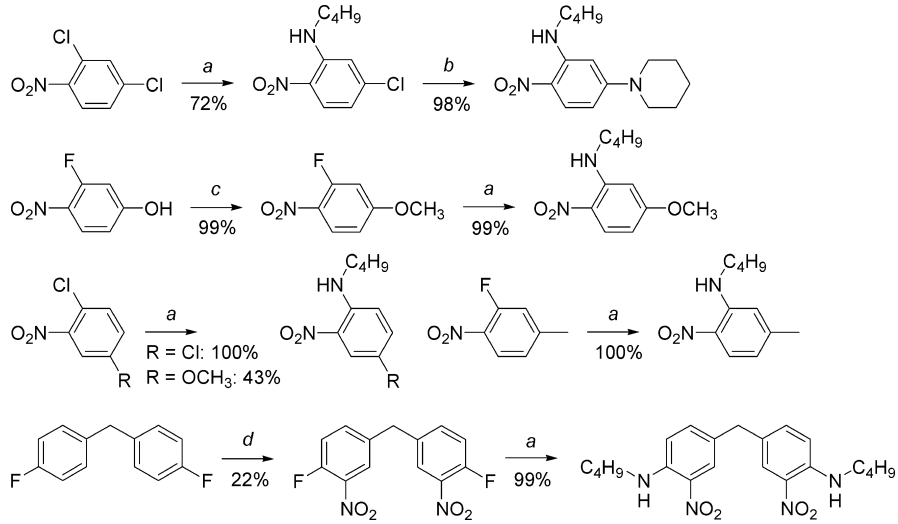

[a] Reaction conditions: (a) *n*-butylamine (excess, used as a reagent and as a base), dry DMSO, under N_2, heating; (b) piperidine (reagent, base and solvent), under N_2, reflux; (c) MeI, K_2CO_3, acetone, in the dark, under N_2, rt; (d) HNO_3 (fuming, $d = 1.5$, reagent and solvent), under air, 0°C.

Chart 2. Structures of the Lanthanide Complexes[a,b]

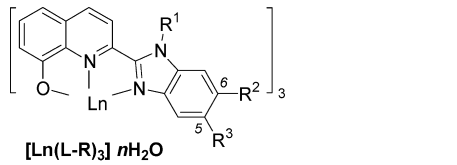

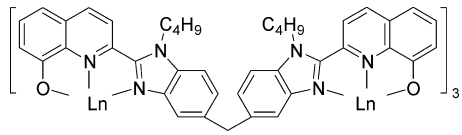

[a] Benzimidazole ring numbering is indicated in the top structure. [b] The structural assignment of lanthanide complexes with bridging bis-tridentate ligand HL2 as binuclear species $[Ln_2(L2)_3]\cdot nH_2O$ is tentative in the absence of X-ray crystallographic characterization.

being bound to one of the three ligands of the same complex, and at the same time, two H_2O molecules being hydrogen-bonded to each other.

The structural assignment of lanthanide complexes with the bridging bis-tridentate ligand HL2 as binuclear species $[Ln_2(L2)_3]\cdot nH_2O$ (Chart 2) is tentative because single crystals suitable for X-ray crystallography could not be grown. This assignment is however supported by the results of elemental analysis which confirms the metal-to-ligand ratio, as well as by ^{1}H NMR and time-resolved luminescence spectroscopy (vide infra), which indicate that the complex is present as a single species in solution and in solid state. It should be noted that the proposed binuclear structure $[Ln_2(L2)_3]$ would require an up−up−up arrangement of the ligands around the metal ions, in contrast to mononuclear complexes $[Ln(L\text{-}R)_3]$ for which the crystal structures show the ligands to be arranged in an up−up−down fashion. The $[Ln_2(L2)_3]$ complex is likely to have a triple-helix structure as was observed for lanthanide complexes with similar bridging ligands.[30]

As discussed in the Synthesis section, we could not obtain pure complexes of the composition $[Ln(L)_3]$ for heavy lanthanides (Er^{III}, Yb^{III}). This may be explained by relatively small ionic radii of these ions (compared to light lanthanides from La^{III} to Gd^{III}) which may prevent coordination of three rigid tridentate ligands $(L)^-$ to a metal center.

^{1}H NMR Spectroscopy of La^{III} Complexes. ^{1}H NMR spectroscopy of diamagnetic La^{III} complexes in CD_2Cl_2 solution provided insight into their solution behavior (Figure S9−S12). The spectra of La^{III} complexes with tridentate ligands in the concentration range $(6.6-24) \times 10^{-4}$ M displayed both signals of coordinated ligand molecules, which were generally broad, and sharp signals of uncoordinated ligand, which increased in relative intensity upon dilution, indicating dissociation of the complexes in CD_2Cl_2 solution (Figures S10−S12).

In contrast, ^{1}H NMR spectra of the complex $[La_2(L2)_3]$ with the bis-tridentate bridging ligand $(L2)^-$ in the concentration range of $(4.4-12) \times 10^{-4}$ M displayed only sharp signals from the coordinated ligands (Figures 2 and S9). These spectra are consistent with the assumed binuclear structure shown in Chart 2. For instance, a single set of signals was observed for the aromatic protons, while the protons of the methylene bridge appeared as a sharp singlet at 3.48 ppm; each of these protons integrating for 2H per ligand, which indicates that the two chelating units of $(L2)^-$ are equivalent on the ^{1}H NMR time scale, as well as all three ligands in the complex. However, protons of the methylene group *N*-*n*-CH_2-C_3H_7 (part of the *n*-butyl chain attached to benzimidazole ring) appeared as two multiplets in the range 4.50−4.35 and 4.20−4.05 ppm, each with intensity of 2H per ligand, instead of a triplet with intensity of 4H as observed in the free ligand. This may indicate a lack of free rotation within the *n*-butyl

(30) (a) Zeckert, K.; Hamacek, J.; Senegas, J.-M.; Dalla-Favera, N.; Floquet, S.; Bernardinelli, G.; Piguet, C. *Angew. Chem., Int. Ed.* **2005**, *44*, 7954. (b) Jensen, T. B.; Scopelliti, R.; Bünzli, J.-C. G. *Chem.—Eur. J.* **2007**, *13*, 8404.

Table 1. Crystal Data and Structure Refinement[a]

compound	HL-CL	[La(L)$_3$]	[Pr(L)$_3$]	[Nd(L)$_3$]	[Sm(L)$_3$]	[Eu(L)$_3$]
empirical formula	$C_{20}H_{18}ClN_3O$	$C_{57}H_{45.50}LaN_{12}O_{3.25}$	$C_{54}H_{48}N_9O_6Pr$	$C_{57}H_{46}N_{12}NdO_{3.50}$	$C_{57}H_{45.50}N_{12}O_{3.25}Sm$	$C_{57}H_{48}EuN_{11}O_4$
fw	351.82	1089.46	1059.92	1099.30	1100.90	1103.02
temp [K]	100(2)	140(2)	100(2)	100(2)	100(2)	140(2)
cryst syst	monoclinic	triclinic	monoclinic	triclinic	triclinic	triclinic
space group	$P2_1/c$	$P\bar{1}$	$P2_1/c$	$P\bar{1}$	$P\bar{1}$	$P\bar{1}$
unit cell dimensions	a = 21.570(4) Å	a = 11.9317(7) Å	a = 15.771(3) Å	a = 11.951(13) Å	a = 11.928(19) Å	a = 11.7570(3) Å
	b = 9.4787(19) Å	b = 12.5460(5) Å	b = 18.094(4) Å	b = 12.621(14) Å	b = 12.587(12) Å	b = 20.2549(5) Å
	c = 16.852(3) Å	c = 18.6060(10) Å	c = 16.589(3) Å	c = 18.559(14) Å	c = 18.504(16) Å	c = 22.1412(6) Å
	α = 90°	α = 78.989(4)°	α = 90°	α = 79.26(8)°	α = 79.31(10)°	α = 67.850(2)°
	β = 99.00(3)°	β = 75.239(5)°	β = 101.61(3)°	β = 75.41(7)°	β = 75.36(11)°	β = 82.513(2)°
	γ = 90°	γ = 66.466(5)°	γ = 90°	γ = 66.70(7)°	γ = 66.77(9)°	γ = 88.846(2)°
vol [Å^3]	3403.1(12)	2456.7(2)	4637.0(16)	2476(4)	2458(5)	4839.5(2)
Z	8	2	4	2	2	4
ρ(calcd) [Mg/m^3]	1.373	1.473	1.518	1.474	1.487	1.514
μ [mm^{-1}]	0.238	0.930	1.115	1.109	1.255	1.358
F(000)	1472	1109	2168	1120	1119	2248
cryst size [mm^3]	0.55 × 0.12 × 0.07	0.19 × 0.13 × 0.12	0.66 × 0.14 × 0.11	0.17 × 0.10 × 0.07	0.15 × 0.07 × 0.03	0.44 × 0.40 × 0.23
θ range	3.47 − 23.26°	2.62 − 25.02°	3.34 − 23.00°	3.30 − 22.98°	3.31 − 24.41°	2.58 − 26.02°
index ranges	$-23 \le h \le 23$	$-14 \le h \le 14$	$-17 \le h \le 17$	$-13 \le h \le 13$	$-13 \le h \le 13$	$-14 \le h \le 14$
	$-10 \le k \le 10$	$-14 \le k \le 14$	$-19 \le k \le 19$	$-13 \le k \le 13$	$-13 \le k \le 14$	$-24 \le k \le 24$
	$-14 \le l \le 18$	$-21 \le l \le 22$	$-18 \le l \le 18$	$-20 \le l \le 20$	$-21 \le l \le 21$	$-27 \le l \le 27$
reflns collected	19 999	18 968	35 040	20 746	31 467	42 376
independent reflns	4685 [R(int) = 0.2571]	8638 [R(int) = 0.0826]	6395 [R(int) = 0.1585]	6701 [R(int) = 0.1451]	7993 [R(int) = 0.1874]	18 929 [R(int) = 0.0472]
completeness to θ	23.26−95.8%	25.02−99.7%	23.00−99.1%	22.98−97.4%	24.41−98.7%	26.02−99.3%
max/min transm		1.00000/0.81702	1.0000/0.5784	1.0000/0.4427	1.0000/0.8209	1.00000/0.77051
data/restraints/params	4685/6/451	8638/12/667	6395/67/643	6701/24/667	7993/0/667	18 929/24/1353
GOF on F^2	1.061	1.120	1.063	1.136	1.166	1.016
final R indices [$I > 2\sigma(I)$]	R1 = 0.1184	R1 = 0.0681	R1 = 0.1011	R1 = 0.0854	R1 = 0.0957	R1 = 0.0580
	wR2 = 0.1723	wR2 = 0.0836	wR2 = 0.1967	wR2 = 0.1160	wR2 = 0.0854	wR2 = 0.1217
R indices (all data)	R1 = 0.2635	R1 = 0.1357	R1 = 0.1758	R1 = 0.1836	R1 = 0.1921	R1 = 0.1003
	wR2 = 0.2237	wR2 = 0.1052	wR2 = 0.2349	wR2 = 0.1448	wR2 = 0.1033	wR2 = 0.1425
largest diff. peak/hole [e/Å^3]	0.410 and −0.419	0.883 and −0.792	1.003 and −1.106	0.850 and −0.843	0.861 and −1.013	4.071 and −1.327

compound	[La(L-Me)$_3$]	[Nd(L-Cl)$_3$]	[Nd(L-OMe)$_3$]	[Nd(L-Cl*)$_3$]	[La(L-OMe*)$_3$]	[Nd(L-OMe*)$_3$]
empirical formula	$C_{67}H_{66}LaN_{11}O_3$	$C_{60}H_{51}Cl_3N_9NdO_3$	$C_{67}H_{66}N_{11}NdO_6$	$C_{64}H_{63}Cl_3N_9NdO_5$	$C_{71}H_{72}LaN_{13}O_6$	$C_{73}H_{75}N_{14}Nd\ O_6$
fw	1212.22	1196.69	1265.55	1288.82	1342.33	1388.71
temp [K]	140(2)	140(2)	100(2)	100(2)	100(2)	140(2)
cryst syst	monoclinic	triclinic	monoclinic	monoclinic	monoclinic	triclinic
space group	$P2_1/c$	$P\bar{1}$	$P2_1/c$	$P2_1/n$	$P2_1/c$	$P\bar{1}$
unit cell dimensions	a = 19.4306(8) Å	a = 13.0964(10) Å	a = 20.044(4) Å	a = 14.564(2) Å	a = 15.996(2) Å	a = 15.6030(5) Å
	b = 25.3001(8) Å	b = 15.0877(12) Å	b = 25.669(5) Å	b = 14.8219(11) Å	b = 23.080(3) Å	b = 15.7296(4) Å
	c = 12.7795(5) Å	c = 16.9417(9) Å	c = 12.337(3) Å	c = 27.391(3) Å	c = 19.235(2) Å	c = 16.1633(4) Å
	α = 90°	α = 66.715(6)°	α = 90°	α = 90°	α = 90°	α = 102.889(2)°
	β = 102.443(4)°	β = 86.990(5)°	β = 107.65(3)°	β = 93.231(11)°	β = 112.348(7)°	β = 100.872(2)°
	γ = 90°	γ = 78.926(7)°	γ = 90°	γ = 90°	γ = 90°	γ = 111.688(3)°
vol [Å^3]	6134.8(4)	3016.7(4)	6048(2)	5903.3(12)	6567.9(14)	3428.59(16)
Z	4	2	4	4	4	2
ρ(calcd) [Mg/m^3]	1.312	1.317	1.390	1.450	1.358	1.345
μ [mm^{-1}]	0.751	1.043	0.921	1.074	0.713	0.820
F(000)	2504	1218	2612	2644	2776	1438
cryst size [mm^3]	0.25 × 0.19 × 0.13	0.33 × 0.30 × 0.26	0.36 × 0.26 × 0.17	0.48 × 0.16 × 0.07	0.91 × 0.41 × 0.40	0.32 × 0.28 × 0.26
θ range for data collection	2.53−26.37°	2.65−25.03°	3.30−22.80°	3.39−25.02°	3.34−26.37°	2.64−26.02°
index ranges	$-24 \le h \le 24$	$-15 \le h \le 15$	$-21 \le h \le 21$	$-17 \le h \le 17$	$-19 \le h \le 19$	$-19 \le h \le 19$
	$-31 \le k \le 31$	$-17 \le k \le 17$	$-27 \le k \le 27$	$-17 \le k \le 17$	$-28 \le k \le 28$	$-18 \le k \le 19$
	$-15 \le l \le 15$	$-20 \le l \le 20$	$-13 \le l \le 13$	$-32 \le l \le 32$	$-23 \le l \le 24$	$-19 \le l \le 19$
reflns collected	51 160	24 196	64 835	77 777	128 986	27 411
independent reflns	12 479 [R(int) = 0.1118]	10 573 [R(int) = 0.1553]	8056 [R(int) = 0.1551]	10 357 [R(int) = 0.1256]	13 322 [R(int) = 0.0603]	13 383 [R(int) = 0.0303]
completeness to θ	26.37−99.6%	25.03−99.2%	22.80−98.2%	25.02−99.4%	26.37−99.4%	26.02−99.0%
max/min transm	1.00000/0.67321	1.00000/0.69441	1.0000/0.5033	1.0000/0.6734	1.0000/0.6976	1.00000/0.92244
data/restraints/params	12 479/0/739	10 573/486/685	8056/27/766	10 357/6/776	13 322/0/820	13 383/0/913
GOF on F^2	1.107	0.952	1.112	1.130	1.164	1.045
final R indices [$I > 2\sigma(I)$]	R1 = 0.0822	R1 = 0.1109	R1 = 0.0754	R1 = 0.0622	R1 = 0.0407	R1 = 0.0313
	wR2 = 0.1327	wR2 = 0.2328	wR2 = 0.1457	wR2 = 0.0939	wR2 = 0.0791	wR2 = 0.0648
R indices (all data)	R1 = 0.1434	R1 = 0.2209	R1 = 0.1256	R1 = 0.1184	R1 = 0.0647	R1 = 0.0457
	wR2 = 0.1523	wR2 = 0.2889	wR2 = 0.1683	wR2 = 0.1105	wR2 = 0.0916	wR2 = 0.0712
largest diff. peak/hole [e/Å^3]	1.011 and −0.792	2.270 and −0.881	1.867 and −1.180	1.060 and −0.920	1.434 and −0.786	0.539 and −0.464

[a] Data in common: wavelength, 0.71073 Å; refinement method, full-matrix least-squares on F^2; abs correction, none for HL-Cl, semi-empirical from equivalents for all other compounds.

chains (i.e., a rigid structure of the complex) so that each of these methylene protons experiences a different environment. Overall, ^{1}H NMR spectra demonstrate that the [La$_2$(L2)$_3$] complex is present in solution as a single nondissociated species and is likely to have a rigid structure with an averaged idealized D_3 symmetry on the

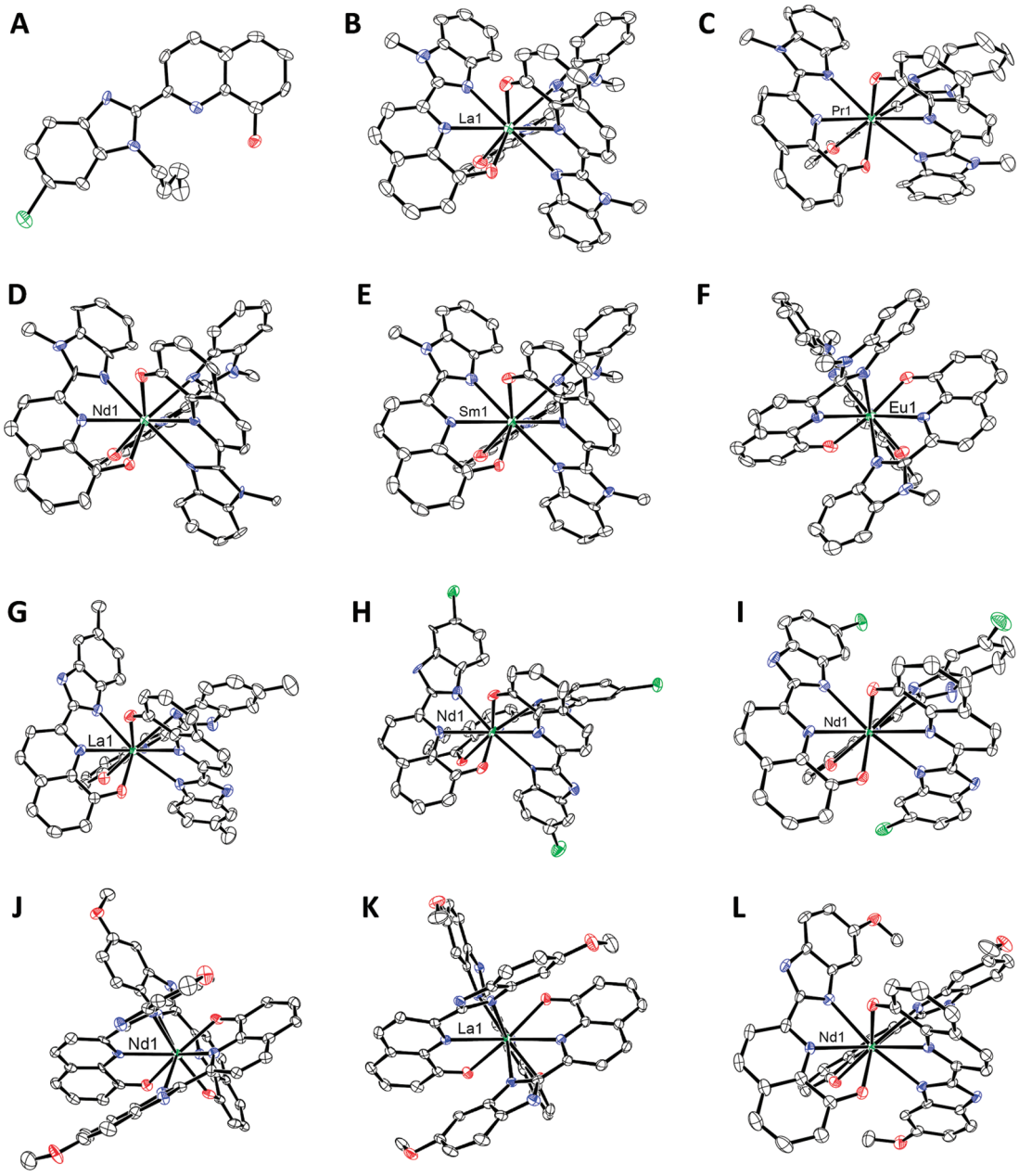

Figure 1. Structures of ligand HL-Cl and lanthanide complexes (50% probability ellipsoids, H atoms, cocrystallized solvent molecules and *N*-*n*-butyl chain on benzimidazole groups omitted). Heteroatom color codes: O, red; N, blue; Cl, bright green; Ln, dark green. From left to right and from top to bottom: HL-Cl (A); $[Ln(L)_3]$ with Ln = La (B), Pr (C), Nd (D), Sm (E), Eu (F); $[La(L\text{-}Me)_3]$ (G); $[Nd(L\text{-}Cl)_3]$ (H); $[Nd(L\text{-}Cl^*)_3]$ (I); $[Nd(L\text{-}OMe)_3]$ (J); $[Ln(L\text{-}OMe^*)_3]$ with Ln = La (K), Nd (L). Only one of the two independent molecules is shown for HL-Cl and $[Eu(L)_3]$. In the complexes, the plane containing the N atoms of the quinoline rings occupying the capping positions of the idealized tricapped trigonal prismatic coordination polyhedron is perpendicular to the plane of the paper.

time scale of ^{1}H NMR experiment. An attempt to perform MALDI-TOF ES mass-spectrometry on this complex in CH_2Cl_2/CH_3CN solution was not entirely successful: although a weak signal assigned to the bis-cation $[La_2(L2)_3]^{2+}$ (m/z =1106.8284, calcd 1107.0775) was observed, other signals at similar m/z ratio (e.g., at m/z = 1121.8191) could not be assigned.

Stability of Ln^{III} Complexes in Solution. The chemical stability of the complexes in dilute solutions used for spectroscopic measurements (4.46−8.40) × 10^{-5} M appeared to depend on the position of the substituent on the benzimidazole ring (all solutions were kept in closed vials in absence of light and under air). For instance, the complexes with ligands modified at position 6 were unstable as indicated by a gradual change of solution color from orange to pale yellow and by the formation of yellow precipitates after 2−5 days. Decomposition is likely to proceed via hydrolysis of the complex by trace amounts of water present in the solvent. At the same time, complexes with ligands modified at position 5 (HL-Cl*, HL-OMe*, and HL2) were relatively more stable, and no color change or precipitate formation was observed within 7 days. However, more concentrated solutions of $[La_2(L2)_3]$ at (4.4−12) × 10^{-4} M in CH_2Cl_2 became turbid in 3−5 days with formation of an orange precipitate, while the solution of the corresponding Nd^{III} complex was stable under the same experimental conditions.

Table 2. Selected Structural Parameters for the Lanthanide Complexes[a]

	bond lengths (Å)[b]			angle (deg)
complex	Ln−O	Ln−N(quin)	Ln−N(bzim)	bzim−quin[c]
[La(L)$_3$]	2.432(5)	2.694(5)	2.731(5)	10.82
	2.438(4)	2.686(5)	2.735(5)	17.52
	2.448(5)	2.730(6)	2.837(5)	25.67
	2.439	**2.703**	**2.767**	**18.00**
[Pr(L)$_3$]	2.388(10)	2.622(12)	2.638(12)	6.65
	2.418(10)	2.696(12)	2.800(12)	21.48
	2.440(10)	2.688(12)	2.847(13)	39.72
	2.415	**2.669**	**2.762**	**22.62**
[Nd(L)$_3$]	2.397(8)	2.637(9)	2.688(10)	11.24
	2.411 (7)	2.619 (9)	2.699 (10)	18.23
	2.410(8)	2.669(9)	2.808 (10)	25.46
	2.406	**2.642**	**2.732**	**18.31**
[Sm(L)$_3$]	2.364(7)	2.622(7)	2.678(7)	11.32
	2.384(6)	2.584(7)	2.678(8)	18.51
	2.377(7)	2.644(8)	2.768(7)	25.64
	2.375	**2.617**	**2.708**	**18.49**
[Eu(L)$_3$] (**1**)[d]	2.353(4)	2.558(5)	2.649(5)	17.49
	2.385(4)	2.587(5)	2.662(5)	12.79
	2.367(4)	2.613(5)	2.723(5)	27.74
	2.368	**2.586**	**2.678**	**19.34**
[Eu(L)$_3$] (**2**)[d]	2.359(4)	2.575(5)	2.649(5)	18.32
	2.354(5)	2.589(6)	2.708(5)	26.54
	2.382(4)	2.603(5)	2.668(5)	11.14
	2.365	**2.589**	**2.675**	**18.67**
[La(L-Me)$_3$]	2.337(4)	2.584(5)	2.704(5)	24.33
	2.374(5)	2.653(6)	2.744(5)	23.21
	2.451(5)	2.642(6)	2.865(6)	44.14
	2.387	**2.626**	**2.771**	**30.56**
[Nd(L-Cl)$_3$]	2.365(10)	2.612(11)	2.656(10)	4.78
	2.343(9)	2.636(10)	2.716(11)	17.37
	2.443(9)	2.725(11)	2.935(11)	40.49
	2.384	**2.658**	**2.769**	**20.88**
[Nd(L-OMe)$_3$]	2.334(6)	2.591(7)	2.697(8)	21.70
	2.380(6)	2.652(8)	2.775(7)	26.63
	2.457(6)	2.650(8)	2.855(7)	41.64
	2.390	**2.631**	**2.776**	**29.99**
[Nd(L-Cl*)$_3$]	2.353(4)	2.593(5)	2.690(5)	7.01
	2.425(4)	2.688(5)	2.703(5)	16.71
	2.431(4)	2.680(5)	2.821(5)	29.26
	2.403	**2.654**	**2.738**	**17.66**
[La(L-OMe*)$_3$]	2.420(2)	2.698(3)	2.748(2)	22.19
	2.451(2)	2.689(3)	2.728(2)	22.37
	2.488(2)	2.757(3)	2.886(3)	30.45
	2.453	**2.714**	**2.787**	**25.00**
[Nd(L-OMe*)$_3$]	2.3756(17)	2.603(2)	2.676(2)	27.33
	2.4083(17)	2.622(2)	2.687(2)	24.26
	2.4084(17)	2.671(2)	2.777(2)	24.62
	2.397	**2.632**	**2.713**	**25.40**

[a] Each line in the table corresponds to *one and the same* ligand in the complex. Numbers in bold are data averaged over the three ligands. [b] N(quin) and N(bzim) are nitrogen atoms of quinoline and benzimidazole rings, respectively. [c] Dihedral angle between planes of quinoline and benzimidazole groups. The planes were defined by C and N atoms of core rings, that is, 10 and 9 atoms for quinoline and benzimidazole rings, respectively. [d] Two independent molecules are present in the unit cell of the [Eu(L)$_3$] complex.

We tentatively assign the instability of the [La$_2$(L2)$_3$] complex in solution to a slow formation of insoluble oligonuclear complexes. Decomposition of all complexes was also encountered during attempted recrystallization from mixed solvents containing ethyl acetate, THF, dioxane, or hexane.

Because of the dissociation or decomposition of most of the complexes in solution, all photophysical experiments were conducted in solid state only, apart from absorption spectroscopy studies, which were carried out in solution to compare spectral properties of ligands and complexes. All solutions used for spectroscopic measurements were freshly prepared before each experiment.

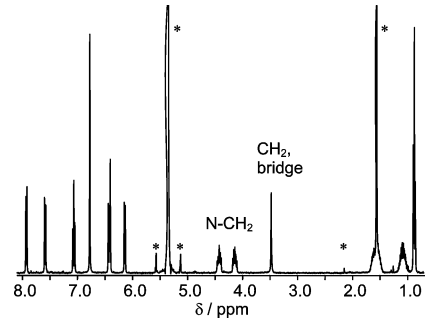

Figure 2. ^{1}H NMR spectrum of complex [La$_2$(L2)$_3$]·3H$_2$O in CD$_2$Cl$_2$ (4.4 × 10^{-4} M). Signals of residual solvents (water, acetone, CH$_2$Cl$_2$) are denoted with (*).

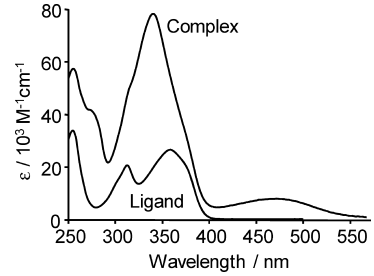

Figure 3. Absorption spectra of the ligand HL-OMe (2.71 × 10^{-4} M) and its Nd^{III} complex (6.78 × 10^{-5} M) in CH$_2$Cl$_2$ solution at room temperature.

Table 3. Absorption Spectra of the Ligands and their Nd^{III} Complexes[a]

compound	λ_{max}/nm (10^{-3} ϵ/M^{-1} cm^{-1})
HL	340 (21), 302 (27), 253 (29)
HL-Cl	343 (25), 306 (28), 256 (33)
HL-Cl*	342 (23), 301 (26), 254 (31)
HL-Me	348 (23), 307 (25), 254 (32)
HL-OMe	359 (26), 312 (20), 255 (34)
HL-OMe*	359 (20), 301 (24), 254 (27)
HL-Pip	386 (23), 321 (9.8), 262 (35)
HL2	352 (48), 304 (49), 253 (61)
[Nd(L-Cl)$_3$]·H$_2$O	481 (7.4), 330 (93), 255 (56)
[Nd(L-Cl*)$_3$]·3H$_2$O	483 (9.0), 330 (99)
[Nd(L-Me)$_3$]·H$_2$O	471 (7.6), 332 (89), 253 (58)
[Nd(L-OMe)$_3$]·H$_2$O	471 (7.2), 340 (78), 255 (57)
[Nd(L-OMe*)$_3$]·3H$_2$O	475 (10), 340 (79)
[Nd(L-Pip)$_3$]·H$_2$O	475 (11, sh), 357 (58), 278 (58), 263 (62)
[Nd$_2$(L2)$_3$]·2H$_2$O	480 (18), 334 (173), 270 (72, sh)

[a] Spectra were recorded in CH$_2$Cl$_2$ solution at rt in the spectral range of 250−800 nm. Estimated errors are ±1 nm for λ_{max} and ±5% for ϵ. The concentration of the samples was in the range (1.14−3.11) × 10^{-4} M for the ligands and (5.36−8.32) × 10^{-5} M for the Nd^{III} complexes. All complexes are likely to be partially dissociated in the concentration range used as indicated by ^{1}H NMR spectroscopy. Complex [Nd(L)$_3$]·2.5H$_2$O was not sufficiently soluble in CH$_2$Cl$_2$ to record its absorption spectrum. The absorption spectra of the La^{III} complexes were nearly identical to the Nd^{III} ones and are given in Table S1.

Absorption Spectroscopy. The UV−vis absorption spectra of the new ligands and their Ln^{III} complexes, recorded in CH$_2$Cl$_2$ solution at room temperature, are shown in Figures 3 and S13−S20, and the main spectral features are summarized in Tables 3 and S1.

The absorption spectra of the ligands display three bands in the spectral range of 250−400 nm; the lowest energy transition is observed at 340−359 nm with absorption cutoff at 400 nm (Figures S13−S19). The only exception is ligand HL-Pip, which is intense yellow in solid state and in solution,

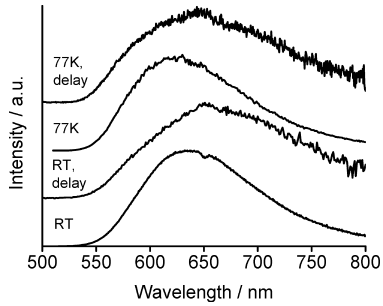

Figure 4. Corrected and normalized luminescence spectra of $[La(L)_3]$ in solid state under air at room temperature or 77 K without or with application of a 10−20 μs time delay; excitation wavelength, 470 nm. The spectra are likely to be distorted because of the presence of self-absorption.

as opposed to white or pale yellow color for the other ligands. Its absorption spectrum contains a low energy band with a maximum at 386 nm and a cutoff at 460 nm (Figure S20). We assign this band to a charge transfer transition located on the benzimidazole ring wherein *N*-piperidyl and *N*-imine groups serve as an electron donor and acceptor, respectively.

Upon deprotonation of the ligand and formation of a lanthanide complex, a new absorption band appears in the visible range with a maximum at 466−483 nm; its molar absorption coefficient is in the range $(7.2-18) \times 10^3$ $M^{-1}cm^{-1}$ (Figures 3 and S14−S20, Tables 3 and S1). This band accounts for an orange or red color of the complexes both in solid state and solution. Its position and intensity are not sensitive to the substitution at the benzimidazole ring, and we assign it to an intraligand phenolate-to-pyridyl charge transfer transition (ILCT) within the 8-hydroxyquinolate chromophore.[2] In fact, the molar absorption coefficient of this band, when calculated per chelating unit is $(2.4-3.7) \times 10^3$ M^{-1} cm^{-1}, which is typical for a metal-coordinated 8-hydroxyquinolate chromophore.[2] Absorption spectra of the La^{III} and Nd^{III} complexes within the spectral range of ligand-centered transitions were nearly identical, as would be expected for this pair of lanthanide ions.

Luminescence of La^{III} Complexes in Solid State. Diamagnetic La^{III} ion lacks metal-centered f-states,[31] and thus its organic complexes display only ligand-centered photophysical processes, often dominated by fluorescence.[4,5] Complexes of La^{III} with benzimidazole-substituted 8-hydroxyquinolines display red luminescence in solid state (Figures 4 and S21−S22). At room temperature, emission maxima are observed at 620−656 nm, and quantum yields are below 2.4%; cooling to 77 K enhances emission intensity and blue-shifts its maximum by 4−12 nm (Table S2). A long-lived component (phosphorescence) is observed in the emission of La^{III} complexes both at room temperature and 77 K (Figures 4 and S22) upon application of a 10−20 μs time delay. All luminescence spectra are broad and featureless at both temperatures and are independent of the excitation wavelength, which was varied from 330−480 nm. The major part of the emission intensity at room temperature is determined by fluorescence with only a small contribution from phosphorescence.

It is interesting to note that for the La^{III} complexes (i) the "blue-edge", and in some cases, the envelope of the phosphorescence band coincides with that of the fluorescence emission (in general, one would expect phosphorescence to be significantly red-shifted compared to fluorescence) (Figure 4); (ii) the emission spectra are not very sensitive to the modification of benzimidazole ring (Figures S21 and S22). To explain these results, we suggest that the lowest ligand-centered excited-state and thus the luminescence properties of the La^{III} complexes are governed by the 8-hydroxyquinolate chromophore. In addition, emission spectra and quantum yield values of the La^{III} complexes in solid state are likely to be distorted by self-absorption of emitted light which results in the apparent "identical" shape and position of fluorescence and phosphorescence spectra (it should be noted that absorption cutoff for the complexes in solution is at 550 nm and would be expected to be further red-shifted in the solid state).

Under the experimental conditions used (room temperature, air, solid-state samples), all La^{III} complexes undergo photodecomposition as evidenced by a gradual loss of emission intensity in series of consecutive experiments (Figure S23). The presence of a reactive long-lived ligand excited-state may explain this photochemical instability (the same excited-state may be responsible for the occurrence of phosphorescence at room temperature in these complexes).

Near Infrared Luminescence of Nd^{III} Complexes in Solid State. The paramagnetic Nd^{III} ion contains an array of f-states,[31,32] which may accept energy from a ligand. As a result, ligand-centered luminescence in the new Nd^{III} complexes is quenched at least 100-fold in comparison to La^{III} complexes. On the other hand, Nd^{III} complexes may display near-infrared emission[15,16] from the metal-centered f-state $^4F_{3/2}$ situated at 11460 cm^{-1}. The energy of the triplet state of the new ligands was estimated to range from about 18 200 to 17 400 cm^{-1} from the onset of the phosphorescence band of the La^{III} complexes (550−575 nm) making these ligands suitable for the sensitization of Nd^{III} emission. Indeed, the Nd^{III} complexes display characteristic metal-centered near-infrared emission from 850 to 1450 nm upon excitation in ligand absorption bands (Figures 5 and S24). The corresponding absolute luminescence quantum yields (Q_L^{Nd}) and lifetimes (τ) in solid state at room temperature are in the range of 0.078−0.34% and 0.35−1.2 μs, respectively, and are typical for Nd^{III} complexes with 8-hydroxyquinolines (Table 4).[6,15] The luminescence decays of Nd^{III} complexes are in all cases single exponential functions, indicating the presence of only one emitting center in solid state. In particular, this observation affirms that the binuclear complex $[Nd_2(L2)_3]$ is likely to be a single species in solid state with equivalent Nd^{III} coordination sites.

(31) Carnall, W. T. The absorption and fluorescence spectra of rare earth ions in solution In *Handbook on the Physics and Chemistry of Rare Earths*; Gschneidner, K. A., Jr., Eyring, L., Eds.; North Holland Publ. Co.: Amsterdam, 1979; Vol. *3*, Chapter 24.

(32) Carnall, W. T.; Fields, P. R.; Rajnak, K. *J. Chem. Phys.* **1968**, *49*, 4424.

(33) Weber, M. J. *Phys. Rev.* **1968**, *171*, 283.

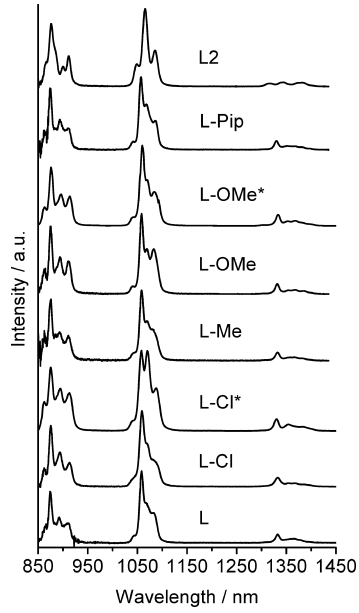

Figure 5. Corrected and normalized luminescence spectra of Nd^{III} complexes in solid state at room temperature. Excitation wavelength, 470 nm (visible absorption band); emission slit, 7 nm; similar spectra were obtained when excitation was performed in UV absorption band at 330−355 nm. The noisy signal observed between 850−875 nm in some spectra is a result of a low sensitivity of NIR detector in this spectral region.

Table 4. Luminescence Properties of Nd^{III} Complexes at Room Temperature in Solid State[a]

complex	$\tau/\mu s$	$Q_L^{Nd}/\%$	$Q_{Nd}^{Nd}/\%^b$	$Q^{ET}/\%^b$
$[Nd(L)_3]\cdot 2.5H_2O$	0.35(3)	0.078	0.13	60
$[Nd(L\text{-}Cl)_3]\cdot H_2O$	1.10(3)	0.18	0.41	44
$[Nd(L\text{-}Cl^*)_3]\cdot 3H_2O$	0.61(3)	0.23	0.23	100
$[Nd(L\text{-}Me)_3]\cdot H_2O$	0.75(3)	0.11	0.28	40
$[Nd(L\text{-}OMe)_3]\cdot H_2O$	1.20(3)	0.26	0.44	59
$[Nd(L\text{-}OMe^*)_3]\cdot 3H_2O$	1.00(6)	0.34	0.37	92
$[Nd(L\text{-}Pip)_3]\cdot H_2O$	1.10(3)	0.15	0.40	37
$[Nd_2(L2)_3]\cdot 2H_2O$	1.01(3)	0.15	0.37	40

[a] $\lambda_{exc} = 355$ nm for τ and 470 nm for Q_L^{Nd}. Estimated error on Q_L^{Nd} is ± 15%. [b] These values were calculated from the equations $Q_L^{Nd} = Q^{ET} \times Q_{Nd}^{Nd}$ and $Q_{Nd}^{Nd} = \tau/\tau_{rad}$ and assuming τ_{rad} (Nd^{III}) as 270 μs.[33] The calculated values of Q^{ET} and Q_{Nd}^{Nd} can only be considered as rough estimates, because they rely on the assumption that $\tau_{rad}(Nd^{III})$ is constant for the entire set of complexes.

The excitation spectra and diffuse reflectance spectra of Nd^{III} complexes in solid state match each other, thus confirming that the ligand sensitizes Nd^{III} luminescence (Figure S25). The Nd^{III} complexes are more photostable compared to La^{III} chelates because of the ability of Nd^{III} to quench the ligand excited states by inducing energy transfer leading to a final excited f-state which is not photoreactive (Figure S26).

The absolute quantum yields of Nd^{III} luminescence upon ligand excitation (Q_L^{Nd}) can be expressed as $Q_L^{Nd} = Q^{ET} \times Q_{Nd}^{Nd}$, where Q^{ET} is the ligand-to-metal energy transfer (sensitization) efficiency and Q_{Nd}^{Nd} is the intrinsic quantum yield of Nd^{III}. An estimate of the intrinsic quantum yield $Q_{Nd}^{Nd} = \tau/\tau_{rad}$ can be made by taking the literature value[33] for the radiative lifetime (τ_{rad}) of Nd^{III} as 270 μs (calculated for Nd^{III} doped in Y_2O_3). These calculations yield Q_{Nd}^{Nd} in the range of 0.13−0.44% and ligand sensitization efficiencies in the range of 37−100% (Table 4). We must stress that the calculated values of Q^{ET} and Q_{Nd}^{Nd} can only be considered as rough estimates because they rely on the assumption that $\tau_{rad}(Nd^{III})$ is constant for the entire set of complexes studied. In fact, $\tau_{rad}(Nd^{III})$ is known to vary significantly in different types of compounds, and literature values employed in similar type of calculations range between 0.25 and 0.8 ms.[15] Thus, calculated estimates of Q^{ET} and Q_{Nd}^{Nd} should be treated with caution, and more credit should be given to the experimentally measured values of Q_L^{Nd} and τ.

The highest values of Q^{ET} of 92% and 100% are observed for ligands substituted at position 5 of benzimidazole ring; however, this trend does not seem to apply to complex $[Nd_2(L2)_3]$. Low sensitization efficiency in the [Nd(L-$NMe_2)_3$] complex may in part have its origin in energy losses within ligand via the intraligand *N*(piperidyl)-to-*N*(imine) charge-transfer state located on a (relatively) weakly coordinated benzimidazole ring (see discussion in Absorption Spectroscopy and X-Ray Crystallography sections).

Because of a small energy gap between emissive and lower lying levels, the $^4F_{3/2}(Nd^{III})$ excited-state is very sensitive to quenching by high-energy vibrations of bonds containing hydrogen atoms, such as O−H, N−H and C−H, even if located at a relatively long distance from the emitting ion.[15,16] However, the quantum yield of Nd^{III} luminescence does not seem to correlate with the number of crystallization water in the samples which varied from 1 to 3. This indicates that these water molecules are interstitial and do not significantly contribute to the quenching of the metal-centered excited state, which is consistent with X-ray crystallography results. Therefore, their contribution to quenching is only a second-sphere effect, possibly assisted by hydrogen-bonding to oxygen atoms of 8-hydroxyquinolate moiety (see discussion in X-Ray Crystallography section).

On the other hand, quenching by vibrations of C−H bonds is expected to play a dominant role because no O−H or N−H groups are directly coordinated to the metal ion. Indeed, replacement of the C−H bond in the ligands with C−N, C−C, C−O, or C−Cl bonds enhances the Nd^{III} luminescence as reflected in the increase of parameters τ, Q_L^{Nd}, and Q_{Nd}^{Nd} (Table 3). The rise in absolute quantum yield Q_L^{Nd} is more pronounced when the C−H bond is removed in position 5 of benzimidazole ring compared to that in position 6 (cf. complexes with ligands HL-Cl*/HL-Cl or HL-OMe*/HL-OMe). This would be expected, considering that the C−H bond at position 5 is situated closer to Nd^{III} and thus has a higher probability of quenching the metal-centered excited state. However, the situation is not that simple because both τ (measured) and Q_{Nd}^{Nd} (calculated) decrease in L-OMe*/L-Cl* versus L-OMe/L-Cl complexes. These two parameters reflect radiative and nonradiative deactivation at the Nd^{III} center, respectively, and indicate that deactivation is increased in L-OMe*/L-Cl* complexes. It appears that the significant increase in Q^{ET} for the L-OMe*/L-Cl* complexes (vide supra) compensates for the decrease in the values of τ and Q_{Nd}^{Nd} resulting in an overall increase of Q_L^{Nd}.

The absolute quantum yields of Nd^{III} complexes, Q_L^{Nd}, decrease in the order L-OMe* > L-OMe > L-Cl* > L-Cl > L2 = L-Pip > L-Me > L. It is of interest to note that substitution of C−H group with C-OCH_3 group was more

beneficial in improving the luminescence efficiency of the Nd^{III} complexes compared to substitution with C−Cl or C−CH_3 group. Both C−OCH_3 and C−CH_3 groups introduce three additional C−H bonds to the ligand. However, C−H oscillators in C−OCH_3 versus the C−CH_3 group are on average situated further apart from Nd^{III} in the complex and are more decoupled from the benzimidazole ring by virtue of the "insulator" C−O bond and thus would be less likely to quench the Nd^{III} excited state. This outcome is reflected in both the Q_L^{Nd} and Q_{Nd}^{Nd} values for Nd^{III} complexes with ligands L-OCH_3 and L-CH_3.

No clearly defined trend could be found between crystallographic parameters (Table 2) and luminescence parameters (Table 4) of the complexes. However, it appears that the most reliable way to improve the luminescence efficiency of Nd^{III} complexes with benzimidazole substituted 8-hydroxyquinoline ligands is by substituting C−H groups in the immediate environment of Nd^{III} with halogen or alkoxy groups.

Finally, we may note that complexes [Ln(L)$_3$] (Ln = Eu, Pr and Sm) do not show luminescence in solid state at room temperature on excitation with UV or visible light. The emissive f-states of these ions ($^5D_1$ and $^5D_0$ for Eu^{III}, $^3P_0$ and $^1D_2$ for Pr^{III}, and $^4G_{5/2}$ for Sm^{III}) are located at relatively high energies (>16 500 cm^{-1}),[19] which is above or similar to the energy of the triplet state of the ligand $(L)^-$. This probably results in fast quenching of excited states of these ions by back-energy transfer to the ligand triplet state.

Conclusions

We have introduced a new class of monoanionic tridentate N,N,O-ligands combining 8-hydroxyquinoline and benzimidazole binding units which form charge-neutral nine-coordinate tris complexes with early lanthanide ions (La^{III}−Eu^{III}). The corresponding Nd^{III} complexes display metal-centered luminescence in the near-infrared spectral region upon UV and visible excitation. The advantages of these ligands are as follows: (i) facile modification of the ligand with a suitable chromophore or an electron-/hole-transport group; (ii) predictable and well-defined structure of the homoleptic complexes with early lanthanide ions; and (iii) presence of an intense ligand-centered visible absorption band for convenient excitation of the lanthanide luminescence. We expect these ligands to be of interest in the design of luminescent materials incorporating near-infrared emitting lanthanides or metal centers with square-planar (Pt^{II}, Pd^{II}) and octahedral (Zn^{II}, Ru^{II}, Os^{II}, Ir^{III}) coordination environment.

Experimental Section

General Methods, Equipment, and Chemicals Used. Elemental analyses were performed by Dr. E. Solari, Service for Elemental Analysis, Institute of Chemical and Chemical Engineering Sciences (EPFL). Absorption spectra were measured on a Perkin-Elmer Lambda 900 UV/vis/NIR spectrometer; ^{1}H NMR spectra (presented as δ in ppm and J in Hz) were recorded on a Bruker Avance DRX 400 MHz spectrometer. Luminescence emission and excitation spectra were measured on a Fluorolog FL 3−22 spectrometer from Horiba-Jobin Yvon-Spex equipped for both visible and NIR measurements. Quantum yield data for solid samples were determined on the same instrument, through an absolute method[34] using a home-modified integrating sphere. Estimated error on values of quantum yields is ±15%. Luminescence lifetimes were measured with a previously described instrumental setup.[18] All luminescence spectra were corrected for the instrumental function. Spectroscopic studies were conducted in freshly prepared solutions in CH_2Cl_2 (Fisher Scientific, analytical reagent grade) using optical cells of 2 mm path length and quartz capillaries with i.d. of 2 mm.

Absorption spectra were recorded at rt in the spectral range of 250−800 nm. Estimated errors are ±1 nm for λ_{max} and ±5% for ϵ. The concentration of the samples was in the range (1.14−3.11) × 10^{-4} M for the ligands, (4.46−8.40) × 10^{-5} M for La^{III} complexes, and (5.36−8.32) × 10^{-5} M for Nd^{III} complexes. All solutions used for spectroscopic measurements were freshly prepared before each experiment.

Chemicals obtained from commercial suppliers were used without further purification: *n*-butylamine (Aldrich), 8-hydroxyquinoline-2-carboxaldehyde (Acros), DMF (absolute, puriss >99.5%, over mol. sieve, Fluka), DMSO (Acros, 99.7%, extra dry, over mol. sieve, water <50 ppm), and 2-methoxyethanol (Fluka, puriss, p.a., >99.5%). Column chromatography was performed on a column with an i.d. of 30 mm using silica gel 60 for preparative chromatography (Fluka, catalogue number 60752). The elution of products was followed on a TLC plate (silica gel 60 F_{254} on aluminum sheets, Merck).

X-Ray Crystallography. Data collections for the 12 crystal structures were performed at low temperature using Mo K_α radiation. An Oxford Diffraction Sapphire/KM4 CCD was employed for [Ln(L)$_3$] (Ln = La, Sm, Eu), [Nd(L-Cl)$_3$], [La(L-Me)$_3$], and [Nd(L-OMe*)$_3$] while the remaining samples were measured on a Bruker APEX II CCD. Both diffractometers have a kappa geometry goniometer. Data were treated by means of either CrysAlis PRO[35] for [Ln(L)$_3$] (Ln = La, Sm, Eu), [Nd(L-Cl)$_3$], [La(L-Me)$_3$], and [Nd(L-OMe*)$_3$] or EvalCCD[36] for the remaining samples; they were then corrected for absorption.[37] Solution and refinement for all structures were performed by SHELXTL.[38] All structures were refined using full-matrix least-squares on F^2 with all non-hydrogen atoms anisotropically defined. Hydrogen atoms were placed in calculated positions by means of the "riding" model. Some of the crystal structures that are shown in this paper display disorder problems (essentially because of solvent or alkyl chains). In two cases ([La(L-Me)$_3$] and [Nd(L-Cl)$_3$]), the SQUEEZE[39] algorithm was used to take into account highly disordered solvent molecules. Another major problem encountered during the refinement of some crystal structures was the anisotropic behavior of some light atoms (mostly carbons). In this case, some restraints (cards ISOR, SIMU, DELU) were applied to get acceptable parameters. Explanations regarding the problems found in the resolution of the structures are given in the Supporting Information.

General Procedure for the Synthesis of Tridentate Ligands (HL, HL-Cl, HL-Pip, HL-Me, HL-OMe, HL-Cl*, HL-OMe*). The synthesis of the precursors is described in the Supporting Information. The reaction was carried out under nitrogen

(34) de Mello, J. C.; Wittmann, H. F.; Friend, R. H. *Adv. Mater.* **1997**, *9*, 230.
(35) *CrysAlis PRO*; Oxford Diffraction Ltd.:Abingdon, Oxfordshire, U.K., 2007.
(36) Duisenberg, A. J. M.; Kroon-Batenburg, L. M. J.; Schreurs, A. M. M. *J. Appl. Crystallogr.* **2003**, *36*, 220.
(37) Blessing, R. H. *Acta Crystallogr., Sect. A* **1995**, *51*, 33.
(38) *SHELXTL*, release 6.1.4; Bruker AXS Inc.: Madison, WI, 2003.
(39) van der Sluis, P.; Spek, A. L. *Acta Crystallogr., Sect. A* **1990**, *46*, 194.

using solvents that were either supplied in degassed form commercially or were degassed by bubbling with nitrogen for 5−10 min. To DMF or 2-methoxyethanol (8 mL) at rt were added substituted *N*-alkyl-2-nitroaniline (1.15 mmol), followed by 2-carboxaldehyde-8-hydroxyquinoline (200 mg, 1.15 mmol). The mixture was stirred until complete dissolution. This was followed by addition of water (2 mL) and solid $Na_2S_2O_4$ (603−635 mg, 3.5−3.65 mmol, >3-molar excess, Riedel-de-Hael, purified, min. 86%). The reaction mixture was sonicated for 5 min at rt and was stirred at 100 °C for 6−8 h under nitrogen to give a yellow to dark brown solution containing a yellow suspension. It was cooled to rt and diluted with water; its pH was checked and, if necessary, adjusted to 5.5−6.5 with aqueous $NaHCO_3$ or acetic acid. It was extracted with ethyl acetate; the organic layer was separated, washed several times with water to remove residues of DMF, and evaporated to dryness. Purification was achieved by column chromatography (25−30 g of silica, 0.3% CH_3OH in CH_2Cl_2 for HL-Cl, 0.5% CH_3OH in CH_2Cl_2 for HL-Pip, 0.4% CH_3OH in CH_2Cl_2 for all other ligands). The fraction containing the product appears as an orange band on the silica column (or orange spot on a TLC plate); the corresponding eluates are colorless, pale yellow or yellow. In most cases the target fraction was either closely preceded or followed by a small amount of intensely colored red, brown, or purple impurity fraction. In all cases, purity of the ligands was checked by TLC (silica, CH_3OH:CH_2Cl_2), by recording ^{1}H NMR spectra in two solvents of different polarity ($CDCl_3$ and DMSO-d_6), and by elemental analysis. Further details on synthesis and purification are provided in the corresponding entries for individual ligands. It should be noted that attempts to perform this reaction at lower temperatures or in the absence of water gave complicated mixtures of products.

Ligand HL. Synthesis was performed in DMF/H_2O with *N*-methyl-2-nitroaniline (175 mg, 1.15 mmol, Acros) as starting material. The pale yellow target fraction was preceded by a small amount of dark red impurity fraction. Pale yellow solid. Yield: 162 mg (0.59 mmol, 51%). Anal. Calcd for $C_{17}H_{13}N_3O$ (MW 275.30): C, 74.17; H, 4.76; N, 15.26. Found: C, 74.23; H, 4.64; N, 14.67. ^{1}H NMR (400 MHz, DMSO-d_6): δ 9.81 (s, br, 1H, OH), 8.50−8.38 (m, 2H), 7.78 (d, J 7.6, 1H), 7.72 (d, *J* 7.6, 1H), 7.55−7.45 (m, 2H), 7.38 (t, *J* 7.2, 1H), 7.31 (t, *J* 7.2, 1H), 7.22 (dd, *J* 7.2, J 1.2, 1H), 4.44 (s, 3H).

Ligand HL-Cl. Synthesis was performed in 2-methoxyethanol/H_2O with 2-*N*-*n*-butylamino-4-chloronitrobenzene (264 mg, 1.15 mmol) as starting material. Pale yellow target fraction coeluted with a small amount of red impurity fraction, which was impossible to separate; the product was pure by ^{1}H NMR analysis. Pale brown or dark yellow solid (coloration is caused by the presence of impurity). Yield: 178 mg (0.51 mmol, 44%). Anal. Calcd for $C_{20}H_{18}ClN_3O$ (MW 351.83): C, 68.28; H, 5.16; N, 11.94. Found: C, 70.56; H, 4.55; N, 11.03. The reason for unsatisfactory element analysis is not known. Crystals suitable for X-ray analysis were obtained by slow evaporation of a CH_2Cl_2/hexane solution of [Nd(L-Cl)$_3$]·H_2O complex via its decomposition (hydrolysis). ^{1}H NMR (400 MHz, DMSO-d_6): δ 10.05 (s, br, 1H, OH), 8.48−8.37 (m, 2H), 7.91 (d, *J* 1.2, 1H), 7.78 (d, J 8.8, 1H), 7.54−7.42 (m, 2H), 7.31 (dd, *J* 8.8, J 1.6, 1H), 7.20 (d, *J* 6.8, 1H), 5.10 (t, *J* 7.6, 2H), 1.77 (p, *J* 7.2, 2H), 1.34 (sextet, *J* 7.6, 2H), 0.83 (t, *J* 7.6, 3H).

Ligand HL-Pip. Synthesis was performed in DMF/H_2O with 2-*N*-*n*-butylamino-4-piperidinonitrobenzene (320 mg, 1.15 mmol) as starting material. The greenish-yellow fluorescent fraction containing the product was collected. The product was obtained as an oil which crystallized when sonicated in hexane. Bright yellow solid. Yield: 184 mg (0.46 mmol, 40%). Anal. Calcd for $C_{25}H_{28}N_4O$ (MW 400.52): C, 74.97; H, 7.05; N, 13.99. Found: C, 75.21; H, 7.55; N, 13.23. ^{1}H NMR (400 MHz, DMSO-d_6): δ 9.83 (s, br, 1H, OH), 8.40−8.35 (m, 2H), 7.57 (d, *J* 8.4, 1H), 7.50−7.38 (m [t + t], 2H), 7.17 (d, J 6.0, 1H), 7.08−7.00 (m [d + dd], 2H), 5.06 (t, J 7.2, 2H), 3.21 (t, *J* 5.6, 4H), 1.76 (p, *J* 7.6, 2H), 1.75−1.65 (m, br, 4H), 1.64−1.52 (m, br, 2H), 1.34 (sextet, *J* 7.6, 2H), 0.83 (t, *J* 7.6, 3H).

Ligand HL-Me. Synthesis was performed in DMF/H_2O with 3-*N*-*n*-butylamino-4-nitrotoluene (240 mg, 1.15 mmol) as starting material. The target fraction coeluted with a small amount of red impurity fraction, which was impossible to separate. The product appeared to be pure by ^{1}H NMR analysis. Pale brown solid. Yield: 246 mg (0.74 mmol, 65%). Anal. Calcd for $C_{21}H_{21}N_3O$ (MW 331.41): C, 76.11; H, 6.39; N, 12.68. Found: C, 76.07; H, 7.05; N, 12.33. ^{1}H NMR (400 MHz, DMSO-d_6): δ 9.94 (s, br 1H, OH), 8.45−8.35 (m, 2H), 7.64 (d, *J* 8.4, 1H), 7.52−7.41 (m, 3H), 7.19 (dd, *J* 7.2, *J* 1.2, 1H), 7.12 (d, *J* 8.0, 1H), 5.07 (t, *J* 7.2, 2H), 1.78 (p, *J* 7.6, 2H), 1.35 (sextet, J 7.6, 2H), 0.84 (t, *J* 7.2, 3H); the signal of the methyl group (s, 3H) was obscured by solvent peak.

Ligand HL-OMe. Synthesis was performed in DMF/H_2O with 2-*N*-*n*-butylamino-4-methoxynitrobenzene (259 mg, 1.15 mmol) as starting material. No complications were encountered during column chromatography. Bright yellow solid. Yield: 263 mg (0.76 mmol, 66%). Anal. Calcd for $C_{21}H_{21}N_3O_2$ (MW 347.41): C, 72.60; H, 6.09; N, 12.10. Found: C, 72.14; H, 6.78; N, 12.02. ^{1}H NMR (400 MHz, DMSO-d_6): δ 9.87 (s, br, 1H, OH), 8.45−8.35 (m, 2H), 7.64 (d, J 8.8, 1H), 7.52−7.41 (m, 2H), 7.22 (d, J 2.4, 1H), 7.19 (dd, J 7.2, J 1.2, 1H), 6.92 (dd, J 8.8, J 2.0, 1H), 5.08 (t, J 7.2, 2H), 3.88 (s, 3H), 1.78 (p, J 7.2, 2H), 1.34 (sextet, J 7.6, 2H), 0.83 (t, J 7.2, 3H).

Ligand HL-OMe*. Synthesis was performed in DMF/H_2O with 2-*N*-*n*-butylamino-5-methoxynitrobenzene (260 mg, 1.16 mmol) as starting material. The target fraction was preceded by a bright purple impurity fraction. Pale purple solid (coloration is caused by an impurity). Yield: 162 mg (0.47 mmol, 40%). Anal. Calcd for $C_{21}H_{21}N_3O_2$ (MW 347.41): C, 72.60; H, 6.09; N, 12.10. Found: C, 72.25; H, 6.26; N, 11.66. ^{1}H NMR (400 MHz, DMSO-d_6): δ 9.97 (s, br, 1H, OH), 8.45−8.37 (m, 2H), 7.61 (d, *J* 8.8, 1H), 7.52−7.41 (m, 2H), 7.28 (d, *J* 2.4, 1H), 7.18 (d, *J* 7.2, 1H), 6.99 (dd, *J* 9.2, *J* 2.4, 1H), 5.07 (t, 2H), 3.83 (s, 3H, OCH_3), 1.77 (p, 2H), 1.33 (sextet, 2H), 0.83 (t, *J* 7.2, 3H).

Ligand HL-Cl*. Synthesis was performed in 2-methoxyethanol/H_2O with 2-*N*-*n*-butylamino-5-chloronitrobenzene (264 mg, 1.15 mmol) as starting material. The target fraction was preceded by pale yellow fraction and followed by dark red fraction containing impurities. Pale yellow solid. Yield: 120 mg (0.34 mmol, 30%). Anal. Calcd for $C_{20}H_{18}ClN_3O$ (MW 351.83): C, 68.28; H, 5.16; N, 11.94. Found: C, 68.23; H, 5.18; N, 11.75. ^{1}H NMR (400 MHz, DMSO-d_6): δ 10.10 (s, br, 1H, OH), 8.48−8.38 (m, 2H), 7.84 (d, *J* 1.6, 1H), 7.79 (d, *J* 8.8, 1H), 7.54−7.42 (m, 2H), 7.38 (dd, *J* 8.4, J 1.6, 1H), 7.20 (d, *J* 7.6, 1H), 5.11 (t, *J* 7.2, 2H), 1.78 (p, *J* 7.2, 2H), 1.33 (sextet, *J* 7.6, 2H), 0.83 (t, *J* 7.2, 3H).

Synthesis of Bridging Bis-Tridentate Ligand HL2. Reaction was carried out under nitrogen using solvents that were degassed by bubbling with nitrogen for 5−10 min. 3,3′-Dinitro-4,4′-di-(*N*-*n*-butylamino)-diphenylmethane (231 mg, 0.57 mmol) and 2-carboxaldehyde-8-hydroxyquinoline (200 mg, 1.15 mmol) were dissolved in DMF (8 mL), followed by addition of water (2 mL) and solid $Na_2S_2O_4$ (603 mg, 3.5 mmol, 3-molar excess). The reaction mixture was sonicated for 5 min at rt and was stirred at 100 °C for 6 h under nitrogen to give brown suspension. It was cooled to rt and diluted with water (>75 mL) its pH checked and adjusted to 5.5−6.5 with aqueous $NaHCO_3$ and acetic acid. The resulting dark yellow suspension was filtered to give brown solid, which was

thoroughly washed with water and ether. Purification was achieved by column chromatography (10−15 g of silica, 0.8% CH_3OH in CH_2Cl_2 to remove impurities and 0.8−0.9% CH_3OH in CH_2Cl_2 to recover the product). The pale yellow fraction containing the product was preceded by red and pale yellow impurity fractions; their separation accounted for a diminished yield. White or pale-yellow solid. Yield: 154 mg (0.24 mmol, 42%). Anal. Calcd for $C_{41}H_{38}N_6O_2$ (MW 646.78): C, 76.14; H, 5.92; N, 12.99. Found: C, 75.93; H, 5.99; N, 12.44. ^{1}H NMR (400 MHz, DMSO-d_6): δ 9.93 (s, br, 2H, OH), 8.46−8.38 (m, 4H), 7.69 (s, 2H), 7.63 (d, *J* 8.4, 2H), 7.52−7.42 (m, 4H), 7.31 (dd, *J* 8.4, *J* 1.2, 2H), 7.19 (dd, *J* 7.2, *J* 1.2, 2H), 5.07 (t, *J* 7.2, 4H), 4.24 (s, 2H), 1.77 (p, *J* 7.2, 4H), 1.32 (sextet, *J* 7.6, 4H), 0.82 (t, *J* 7.6, 6H). ^{1}H NMR (400 MHz, CD_2Cl_2): δ 8.60 (d, *J* 8.8, 2H), 8.36 (d, *J* 8.4, 2H), 7.85 (s, 2H), 7.74 (s, 2H), 7.56 (t, *J* 8.0, 2H), 7.51−7.44 (m, 4H), 7.34 (dd, *J* 8.4, *J* 1.6, 2H), 7.26 (dd, *J* 7.6, *J* 1.2, 2H), 4.87 (t, *J* 7.6, 4H), 4.34 (s, 2H), 2.05 (p, *J* 7.6, 4H), 1.50 (sextet, *J* 8.0, 4H), 0.99 (t, *J* 7.6, 6H).

Synthesis of the Ln^{III} Complexes. Synthesis of all Ln^{III} complexes was carried out under air. Solutions of neutral ligands in ethanol are colorless or pale yellow but turn bright orange or red upon deprotonation.

Although elemental analysis suggested presence of up to 3 molecules of water per lanthanide complex, no coordinated water molecules were observed in the X-ray structures. Thus we conclude that these were interstitial and not coordinated water molecules.

All complexes, except $[LnL_3]\cdot nH_2O$, were well soluble in CH_2Cl_2 and to a lesser extent in $CHCl_3$. The $[LnL_3]\cdot nH_2O$ complexes were rather insoluble in most organic solvents, including CH_2Cl_2. All complexes were soluble to some extent in boiling acetonitrile and boiling ethanol, were less soluble or insoluble in boiling isopropanol, and were insoluble in water, water/ethanol (50:50), hexane, and ether. Further details are provided in the corresponding entries for individual complexes.

All spectroscopic measurements were conducted with the samples of Ln^{III} complexes obtained directly from the synthesis and used without any further purification. To grow single crystals for X-ray crystallographic analysis, a small sample (1−2 mg) of the complex was recrystallized from a suitable solvent or a mixture of solvents (solutions were always kept in dark during recrystallizations). It was noted that in many cases, acetonitrile when used either as a recrystallization solvent or as a cosolvent was beneficial to the growth of good quality single crystals.

Synthesis of $[LnL_3]\cdot nH_2O$ (Ln = La^{III}, Pr^{III}, Nd^{III}, Sm^{III}, Eu^{III}, Gd^{III}). Ligand HL (50 mg, 0.182 mmol) and NaOH (7.26 mg, 0.182 mmol; in 0.5 mL of water) were dissolved in hot ethanol (5 mL) to give a red solution. A solution of $LnCl_3\cdot nH_2O$ (0.0605 mmol) in ethanol (2 mL) was added dropwise. Upon addition, the color of reaction mixture changed to deep red, and a dark red precipitate formed. The suspension was stirred for 15 min at 70−80 °C and cooled to rt. The precipitate was filtered and thoroughly washed with ethanol/water (50:50) and ether. In the case of La^{III}−Gd^{III} ions, the precipitate was compact and well formed, while in the case of Er^{III} and Yb^{III} the precipitate was amorphous and voluminous. The La^{III}−Eu^{III} complexes (when freshly precipitated from ethanol/water solution) were completely soluble in hot CH_3CN, while the Gd^{III} complex was less soluble. Upon recrystallization from hot acetonitrile solution (to get single crystals for X-ray analysis), it was noted that La^{III}−Eu^{III} complexes provided crystals of uniform size, shape, and color and left a colorless supernatant solution, while the Gd^{III} complex gave a mixture of very small red crystals and yellow amorphous material. The crystals of La^{III}−Eu^{III} complexes obtained after recrystallization from acetonitrile could not be dissolved again in acetonitrile. All complexes were dark orange solids.

$[LaL_3]\cdot 3H_2O$. Yield: 54 mg (0.053 mmol, 88%). Anal. Calcd for $C_{51}H_{36}LaN_9O_3\cdot 3H_2O$ (MW 1015.84): C, 60.30; H, 4.17; N, 12.41. Found: C, 60.52; H, 3.59; N, 11.74. Single crystals for X-ray analysis were obtained by cooling hot solution of the complex in CH_3CN to rt and keeping it at rt for a few days in a closed vial. In one of the synthetic preparations conducted at higher dilution, no precipitate was observed from the hot ethanol/water solution upon mixing of reagents, but a crystalline solid appeared on slow cooling to rt; the quality of crystals seemed to be suitable for X-ray analysis. These crystals were initially orange, but on drying under vacuum changed color to deep-red. Element analysis for the "single crystalline" batch and its assignment were as follows. Anal. Calcd for $C_{51}H_{36}LaN_9O_3\cdot 2H_2O$ (MW 997.83): C, 61.39; H, 4.04; N, 12.63. Found: C, 61.57; H, 3.84; N, 12.15.

$[PrL_3]\cdot 3H_2O$. Yield: 56 mg (0.055 mmol, 91%). Anal. Calcd for $C_{51}H_{36}N_9O_3Pr\cdot 3H_2O$ (MW 1017.84): C, 60.18; H, 4.16; N, 12.39. Found: C, 60.04; H, 4.06; N, 11.82. Single crystals were grown by cooling of the hot solution of the complex in CH_3CN/C_2H_5OH/*i*-C_3H_7OH to rt followed by slow evaporation.

$[NdL_3]\cdot 2.5H_2O$. Yield: 55 mg (0.054 mmol, 90%). Anal. Calcd for $C_{51}H_{36}N_9NdO_3\cdot 2.5H_2O$ (MW 1012.17): C, 60.52; H, 4.08; N, 12.45. Found: C, 60.29; H, 3.75; N, 11.55. Single crystals were grown by cooling of hot solution of the complex in CH_3CN to rt and keeping it at rt for a few days in a closed vial.

$[SmL_3]\cdot 3H_2O$. Yield: 52 mg (0.051 mmol, 84%). Anal. Calcd for $C_{51}H_{36}N_9O_3Sm\cdot 3H_2O$ (MW 1027.30): C, 59.63; H, 4.12; N, 12.27. Found: C, 59.75; H, 4.38; N, 11.28. Single crystals were grown by cooling of a hot solution of the complex in CH_3CN to rt, followed by slow evaporation.

$[EuL_3]\cdot 3H_2O$. Yield: 56 mg (0.054 mmol, 90%). Anal. Calcd for $C_{51}H_{36}EuN_9O_3\cdot 3H_2O$ (MW 1028.90): C, 59.53; H, 4.11; N, 12.25. Found: C, 59.86; H, 4.08; N, 11.62. Single crystals were grown by cooling of hot solution of the complex in CH_3CN/C_2H_5OH/*i*-C_3H_7OH to rt and keeping it at rt for a few days in a closed vial.

$[GdL_3]\cdot 3H_2O$. Yield: 55 mg (0.053 mmol, 88%). Anal. Calcd for $C_{51}H_{36}GdN_9O_3\cdot 3H_2O$ (MW 1034.19): C, 59.23; H, 4.09; N, 12.19. Found: C, 59.46; H, 4.21; N, 11.54. Single crystals of good quality could not be grown, and thus the structure of the complex could not be confirmed by X-ray analysis.

Attempts to isolate pure Er^{III} and Yb^{III} complexes of the composition $[LnL_3]\cdot nH_2O$ failed. The following analytical results were obtained for these solids. Er^{III} complex. Yield: 16 mg. Anal. Found: C, 57.35; H, 3.06; N, 11.46. Yb^{III} complex. Yield: 31 mg. Anal. Found: C, 56.68; H, 3.28; N, 11.33.

Synthesis of $[Ln(L\text{-}Cl)_3]\cdot H_2O$ (Ln = La^{III}, Nd^{III}). Ligand HL-Cl (50 mg, 0.142 mmol) and NaOH (5.68 mg, 0.142 mmol; in 0.5 mL of water) were dissolved in hot ethanol (5 mL) to give a red solution. A solution of $LnCl_3\cdot nH_2O$ (0.047 mmol) in ethanol (2 mL) was added dropwise. Upon addition, the color of reaction mixture changed to red, and a small amount of red precipitate formed. Additional water (4 mL) was added dropwise to the hot reaction mixture to complete precipitation of the product. The suspension was stirred for 15 min at 70−80 °C and cooled to rt. The precipitate was filtered and thoroughly washed with ethanol/water (50:50) and ether. The two complexes were red solids.

[La(L-Cl)$_3$]·H$_2$O. Yield: 42 mg (0.035 mmol, 74%). Anal. Calcd for $C_{60}H_{51}Cl_3LaN_9O_3 \cdot H_2O$ (MW 1209.39): C, 59.59; H, 4.42; N, 10.42. Found: C, 59.32; H, 4.45; N, 9.94.

[Nd(L-Cl)$_3$]·H$_2$O. Yield: 46 mg (0.038 mmol, 81%). Anal. Calcd for $C_{60}H_{51}Cl_3N_9NdO_3 \cdot H_2O$ (MW 1214.72): C, 59.33; H, 4.40; N, 10.38. Found: C, 59.55; H, 4.48; N, 9.94. Single crystals were grown by evaporation of an ethanol solution.

Synthesis of [Ln(L-Pip)$_3$]·H$_2$O (Ln = La^{III}, Nd^{III}). Ligand HL-Pip (60 mg, 0.15 mmol) and NaOH (5.99 mg, 0.15 mmol; in 0.5 mL of water) were dissolved in hot ethanol (5 mL) to give a dark orange solution. A solution of $LnCl_3 \cdot nH_2O$ (0.05 mmol) in ethanol (2 mL) was added dropwise. Upon addition, the color of the reaction mixture changed to reddish-orange, but no precipitate formed. An additional amount of water (3 mL) was added dropwise to the hot reaction mixture to precipitate the product. The suspension was stirred for 15 min at 70−80 °C and cooled to rt. The precipitate was filtered and thoroughly washed with ethanol/water (50:50) and ether. The two complexes were dark-orange solids.

[La(L-Pip)$_3$]·H$_2$O. Yield: 56 mg (0.041 mmol, 83%). Anal. Calcd for $C_{75}H_{81}LaN_{12}O_3 \cdot H_2O$ (MW 1355.45): C, 66.46; H, 6.17; N, 12.40. Found: C, 66.35; H, 6.03; N, 11.85.

[Nd(L-Pip)$_3$]·H$_2$O. Yield: 59 mg (0.043 mmol, 87%). Anal. Calcd for $C_{75}H_{81}N_{12}NdO_3 \cdot H_2O$ (MW 1360.78): C, 66.20; H, 6.15; N, 12.35. Found: C, 65.74; H, 6.42; N, 12.04.

Synthesis of [Ln(L-Me)$_3$]·H$_2$O (Ln = La^{III}, Nd^{III}). Ligand HL-Me (50 mg, 0.15 mmol) and NaOH (6.03 mg, 0.15 mmol; in 0.5 mL of water) were dissolved in hot ethanol (5 mL) to give a dark orange solution. A solution of $LnCl_3 \cdot nH_2O$ (0.05 mmol) in ethanol (2 mL) was added dropwise. Upon addition, the color of the reaction mixture changed to red, but no precipitate formed. Additional water (5 mL) was added dropwise to hot reaction mixture to precipitate the product. The suspension was stirred for 15 min at 70−80 °C and was cooled to rt. The precipitate was filtered and thoroughly washed with ethanol/water (50:50) and ether. The two complexes were orange solids.

[La(L-Me)$_3$]·H$_2$O. Yield: 50 mg (0.044 mmol, 87%). Anal. Calcd for $C_{63}H_{60}LaN_9O_3 \cdot H_2O$ (MW 1148.13): C, 65.90; H, 5.44; N, 10.98. Found: C, 66.06; H, 5.85; N, 10.93. Single crystals were grown by cooling a hot solution of the complex in CH_3CN to rt, followed by slow evaporation. ^{1}H NMR spectra of the complex in CD_2Cl_2 were broad and concentration-dependent in the range studied (8.7−24) × 10^{-4} M and featured sharp signals of noncoordinated ligand which diminished in relative intensity in more concentrated solutions.

[Nd(L-Me)$_3$]·H$_2$O. Yield: 50 mg (0.043 mmol, 87%). Anal. Calcd for $C_{63}H_{60}N_9NdO_3 \cdot H_2O$ (MW 1153.46): C, 65.60; H, 5.42; N, 10.93. Found: C, 65.66; H, 5.87; N, 10.76.

Synthesis of [Ln(L-OMe)$_3$]·H$_2$O (Ln = La^{III}, Nd^{III}). Ligand HL-OMe (50 mg, 0.144 mmol) and NaOH (5.76 mg, 0.144 mmol; in 0.5 mL of water) were dissolved in hot ethanol (5 mL) to give a dark orange solution. A solution of $LnCl_3 \cdot nH_2O$ (0.048 mmol) in ethanol (2 mL) was added dropwise. Upon addition, the color of reaction mixture changed to bright red, but no precipitate formed. An additional amount of water (2.5 mL) was added dropwise to the hot reaction mixture to precipitate the product. The suspension was stirred for 15 min at 70−80 °C and cooled to rt. The precipitate was filtered and thoroughly washed with ethanol/water (50:50) and ether. The two complexes were bright red solids.

[La(L-OMe)$_3$]·H$_2$O. Yield: 46 mg (0.0385 mmol, 80%). Anal. Calcd for $C_{63}H_{60}LaN_9O_6 \cdot H_2O$ (MW 1196.13): C, 63.26; H, 5.22; N, 10.54. Found: C, 63.45; H, 5.65; N, 10.61.^{1}H NMR spectra of the complex in CD_2Cl_2 were broad and concentration-dependent in the range studied (8.4−23) × 10^{-4} M and featured sharp signals of noncoordinated ligand which diminished in relative intensity in more concentrated solutions.

[Nd(L-OMe)$_3$]·H$_2$O. Yield: 47 mg (0.039 mmol, 81%). Anal. Calcd for $C_{63}H_{60}N_9NdO_6 \cdot H_2O$ (MW 1201.46): C, 62.98; H, 5.20; N, 10.49. Found: C, 63.28; H, 5.37; N, 10.35. Single crystals were grown by cooling a hot solution of the complex in CH_3CN to rt, followed by slow evaporation.

Synthesis of [Ln(L-OMe*)$_3$]·*n*H$_2$O (Ln = La^{III}, Nd^{III}). Ligand HL-OMe* (50 mg, 0.144 mmol) and NaOH (5.76 mg, 0.144 mmol; in 0.5 mL of water) were dissolved in hot ethanol (5 mL) to give dark orange solution. A solution of $LnCl_3 \cdot nH_2O$ (0.048 mmol) in ethanol (2 mL) was added dropwise. Upon addition, the color of reaction mixture changed to bright red, but no precipitate formed. An additional amount of water (4.5 mL) was added dropwise to the hot reaction mixture to precipitate the product. The suspension was stirred for 15 min at 70−80 °C and cooled to rt. The precipitate was filtered and thoroughly washed with ethanol/water (50:50) and ether. The two complexes were bright red solids.

[La(L-OMe*)$_3$]·2H$_2$O. Yield: 46 mg (0.0379 mmol, 79%). Anal. Calcd for $C_{63}H_{60}LaN_9O_6 \cdot 2H_2O$ (MW 1214.14): C, 62.32; H, 5.31; N, 10.38. Found: C, 62.38; H, 5.29; N, 10.05.^{1}H NMR spectra of the complex in CD_2Cl_2 in the concentration range (6.6−21) × 10^{-4} M contained sharp signals in the aromatic region and broad signals in the aliphatic region. The number of observed signals indicated that the ligands were not equivalent. The complex was partially dissociated, as shown by the presence of sharp signals of noncoordinated ligand, which diminished in relative intensity in more concentrated solutions. Single crystals were grown by cooling a hot solution of the complex in CH_3CN to rt and keeping it in a closed vial at rt for a few days.

[Nd(L-OMe*)$_3$]·3H$_2$O. Yield: 50 mg (0.040 mmol, 84%). Anal. Calcd for $C_{63}H_{60}N_9NdO_6 \cdot 3H_2O$ (MW 1237.49): C, 61.15; H, 5.38; N, 10.19. Found: C, 61.35; H, 5.36; N, 9.80. Single crystals were grown by cooling a hot solution of the complex in CH_3CN to rt and keeping it in a closed vial at rt for a few days.

Synthesis of [Nd(L-Cl*)$_3$]·3H$_2$O. Ligand HL-Cl* (50 mg, 0.142 mmol) and NaOH (5.68 mg, 0.142 mmol; in 0.5 mL of water) were dissolved in hot ethanol (5 mL) to give a red solution. A solution of $NdCl_3 \cdot 6H_2O$ (17 mg, 0.047 mmol) in ethanol (2 mL) was added dropwise. Upon addition, the color of reaction mixture changed to red but no precipitate formed. An additional amount of water (2.5 mL) was added dropwise to the hot reaction mixture to precipitate the product. The suspension was stirred for 15 min at 70−80 °C and cooled to rt. The precipitate was filtered and thoroughly washed with ethanol/water (50:50) and ether. Red solid. Yield: 50 mg (0.040 mmol, 85%). Anal. Calcd for $C_{60}H_{51}Cl_3N_9NdO_3 \cdot (H_2O)_3$ (MW 1250.75): C, 57.62; H, 4.59; N, 10.08. Found: C, 57.84; H, 4.43; N, 9.63. Single crystals were obtained by cooling a hot ethanol solution of the complex to rt and keeping it in a closed vial at rt for a few days.

Synthesis of [Ln$_2$(L2)$_3$]·*n*H$_2$O (Ln = La^{III}, Nd^{III}). Ligand HL2 (50 mg, 0.077 mmol) and NaOH (6.18 mg, 0.1545 mmol; in 0.5 mL of water) were dissolved in hot ethanol (5 mL) to give a dark orange solution. A solution of $LnCl_3 \cdot nH_2O$ (0.0515 mmol) in ethanol (2 mL) was added dropwise. Upon addition, the color of reaction mixture changed to bright red, and a small amount of precipitate formed, which dissolved under further stirring. The reaction was stirred for 5 min at 70−80 °C, followed by a slow dropwise addition of water (3.5 mL) to precipitate the product. The suspension was stirred for 15 min at 70−80 °C and cooled to rt. The precipitate was filtered and thoroughly washed with ethanol/water (50:50) and ether. The solid changed color from orange to

bright-red upon washing with ether. The two complexes were bright red solids that were soluble in CH_2Cl_2 and insoluble in chloroform. The proposed structure is tentative because suitable crystals for X-ray analysis could not be grown. MALDI-TOF ES MS (CH_2Cl_2/CH_3CN): $[La_2(L\text{-}2)_3]^{2+}$ (weak signal, m/z =1106.8284, calcd 1107.0775); other minor signals at similar m/z ratios (e.g., at m/z = 1121.8191) could not be interpreted.

$[La_2(L2)_3]\cdot 3H_2O$. Yield: 47 mg (0.0207 mmol, 81%). Anal. Calcd for $C_{123}H_{108}La_2N_{18}O_6\cdot 3H_2O$ (MW 2266.15): C, 65.19; H, 5.07; N, 11.13. Found: C, 65.15; H, 5.34; N, 10.94. ^{1}H NMR (400 MHz, CD_2Cl_2): (number of protons per ligand) 7.93 (d, *J* 8.4, 2H), 7.59 (d, *J* 8.4, 2H), 7.07 (t, *J* 8.0, 2H), 6.78 (s, 4H), 6.46−6.38 (m, 4H), 6.14 (d, *J* 7.2, 2H), 4.50−4.35 (m, 2H), 4.20−4.05 (m, 2H), 3.48 (s, 2H), 1.70−1.45 (two multiplets partially obscured by the signal of water, 2 × 2H), 1.20−0.95 (m, 4H), 0.88 (t, *J* 7.2, 6H). ^{1}H NMR spectra were sharp, unchanged in the concentration range $(4.4-12)\times 10^{-4}$ M and did not feature signals of unbound ligand. The complex was not sufficiently soluble in $CDCl_3$ to record its ^{1}H NMR spectrum and its temperature dependence.

$[Nd_2(L2)_3]\cdot 2H_2O$. Yield: 50 mg (0.022 mmol, 86%). Anal. Calcd for $C_{123}H_{108}N_{18}Nd_2O_6\cdot 2H_2O$ (MW 2258.80): C, 65.40; H, 5.00; N, 11.16. Found: C, 65.12; H, 5.31; N, 11.06.

Acknowledgment. This research is supported by a grant from the Swiss National Science Foundation.

Supporting Information Available: Synthesis of all precursors, ^{1}H NMR spectra of all ligands (Figures S1−S8) and selected La^{III} complexes (Figures S9−S12), absorption spectra of ligands and their complexes (Figures S13−S20), spectroscopic properties of La^{III} complexes (Tables S1, S2), luminescence spectra of La^{III} and Nd^{III} complexes (Figures S21−S22 and S24, respectively), diffuse reflectance spectrum and excitation spectrum of complex [Nd(L-OMe)$_3$] (Figure S25), and photostability of La^{III} and Nd^{III} complexes (Figures S23 and S26 respectively), and a list of explanations regarding the problems highlighted in the checkCIF report.This material is available free of charge via the Internet at http://pubs.acs.org.

IC8010585